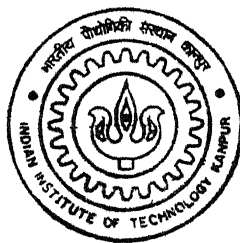# FINITE ELEMENT ANALYSIS BASED DESIGN OF STIFFENED PLATES

by

V. Swaminathan

DEPARTMENT OF AEROSPACE ENGINEERING
INDIAN INSTITUTE OF TECHNOLOGY, KANPUR

February, 2001

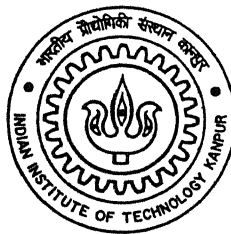# FINITE ELEMENT ANALYSIS BASED DESIGN OF STIFFENED PLATES

A thesis Submitted

in Partial fulfilment of the Requirements

for the Degree of

Master of Technology

by

V.Swaminathan

to the

DEPARTMENT OF AEROSPACE ENGINEERING

INDIAN INSTITUTE OF TECHNOLOGY, KANPUR

February 2001
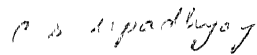
CERTIFICATE

It is certified that work contained in this thesis titled **Finite element analysis based design of stiffened plates** , by **V.Swaminathan**, has been carried out under my supervision and that this work has not been submitted elsewhere for a degree.

Dr. C. S. Upadhyay

Assistant Professor

Department of Aerospace Engineering

Indian Institute of Technology

Kanpur

February 2001.

ABSTRACT

This work presents a method for obtaining optimal topology for stiffened plate structure. The method is based on a combination of existing finite element methods and evolutionary structural optimisation methods. Once the initial finite element problem is defined, the method proceeds by finding recovered smoothened stress field througout the structure and the elements are subdivided into subelements inorder to improve the accuracy of identification of the low stressed material. Low stressed regions are identified in the stiffened layer and remeshing is done seperately in each regions. The elements in the low stressed regions are removed by decreasing the material properties to near zero and this evolved structure is solved. The process is repeated by increasing the lower stress limit for plotting low stressed regions in each iteration, until the stopping criterion is reached. The results produced are presented and its advantages are highlighted.

ACKNOWLEDGEMENTS

I take this opportunity to express my immense gratitude and sincere thanks to my thesis supervisor Dr. C. S. Upadhyay for his constant support and guidance throughout this work.His deep involvement throughout this work,easy availability even on weekends helped me to complete this work successfully.I thank him for given me full freedom and the patience to see me in tough days of my thesis.A word of thanks or gratitude is not sufficient to express my feelings for all he has done to me.

I am thankful to all of my friends and well wishers for making my stay at IIT-Kanpur a memorable experience.

Words are not enough to explain my feelings towords my Parents and my sisters, they have always been the constant source of moral encouragement to me.

<div align="right">V.Swaminathan.</div>

Contents

List of Figures

iv

List of Tables

LIST OF SYMBOLS

x, y, z	Cartesian coordinates
X, Y, t	Length, width and thickness of the plate
N_l	Number of layers
h_i	Thickness of ith lamina
α_i	Orientation of ith lamina
$\{\delta\}$	Generalized displacement vector
Q_i	Material stiffness matrix for i^{th} lamina
$\bar{Q}_i$	Transformed material stiffness matrix for i^{th} lamina
N_x, N_y, N_{xy}	Stress resultants
M_x, M_y, M_{xy}	Moment resultants
M_x^*, M_y^*, M_{xy}^*	Moment resultants
Q_x, Q_y	Shear stress resultants
Q_x^*, Q_y^*	Shear stress resultants
D_m	Membrane rigidity matrix
D_b	Flexure rigidity matrix
D_c	Coupling rigidity matrix
D_s	Shear rigidity matrix
D	Overall rigidity matrix
ϵ_0	Mid surface strains
k_x, k_y	Mid surface curvatures
k_x^*, k_y^*, ν, ν^*	Higher order terms
U	Potential energy
$[K]$	Stiffness matrix
W	Weight of the laminate
$\bar{N}_x, \bar{N}_y, \bar{N}_{xy}$	Applied inplane loads

Chapter 1

INTRODUCTION

1.1 GENERAL

Rapid progress in computer hardware has opened new vistas for structural analysis and design. Large-scale problems with high requirements of in-core and out-of-core memory and processing speed have become tractable even on a PC. One such problem is that of structural optimization. This has been a topic of interest for many years, but has seen a recent resurgence with the rapid progress made by computer hardware. Typically, structural optimization was restricted to truss or frame type structures and laminated composites(lay-up, cut-out shape optimization).

Topology optimization is a recent research topic, with a goal to start from a "slab" of material and "carve" out the final optimal design from it. This can lead to opening of new holes (i.e changing the topology) and "shaping" of existing holes in a structure, to lead to a fully stressed structure [4]. For example, let us consider the beam given in Fig.1.1(a) and Fig.1.1(b). Starting from a solid beam, with the loading shown, material was removed iteratively to reach the final hollow beam configuration shown. Here it was required that the beam does not buckle under the applied(constant) axial load, and the Mises stress at any point does not exceed eighty percent of the yield stress. From the figure we note that the amount of

1
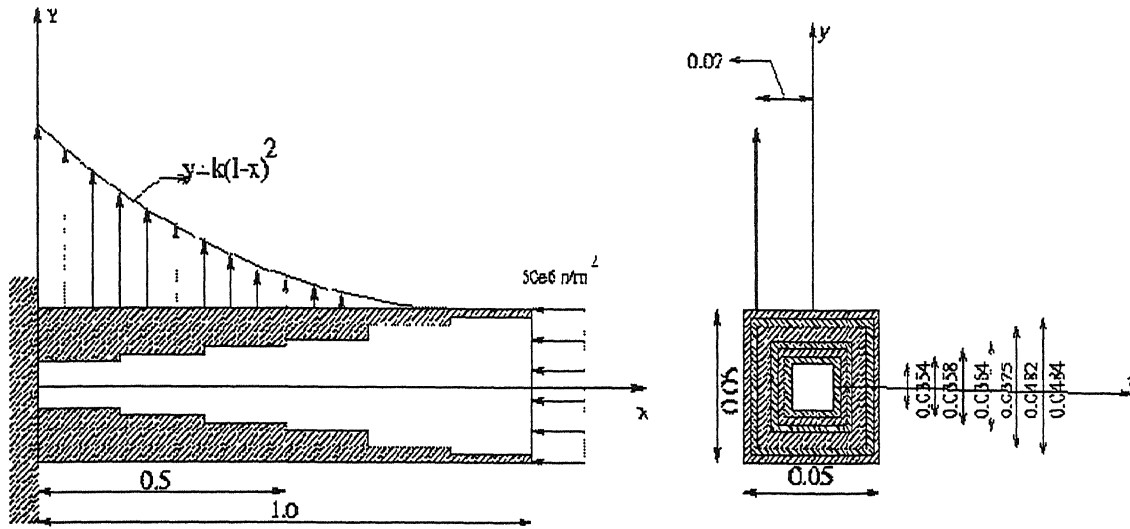
EFFICIENCY OF MATERIAL REMOVAL IS 66.7384%   (volume of material removed / initial volume)
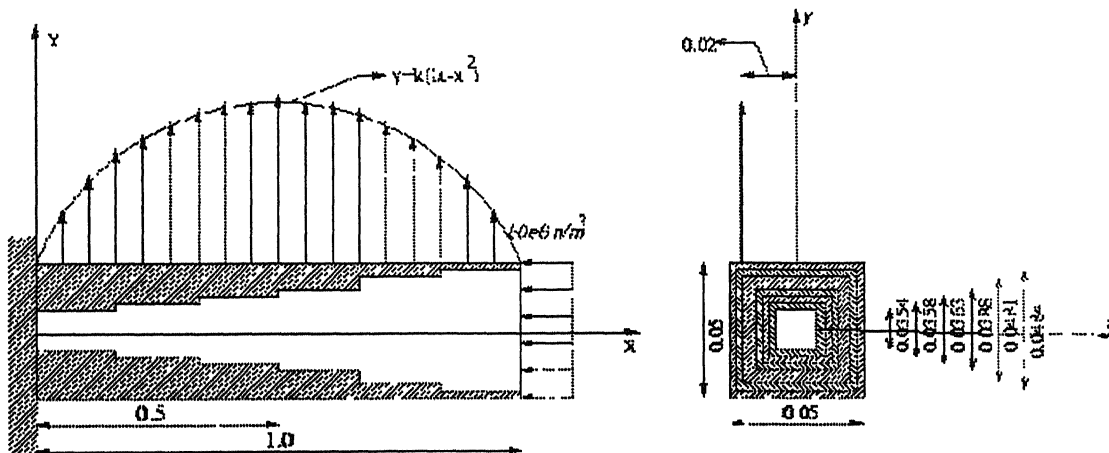
EFFICIENCY OF MATERIAL REMOVAL IS 66.7668%

NOTE: In first step removal critical buckling load is kept as 1.3*applied compressive load. In the following steps 1.3 is reduced by steps of (0.3)/5, so that in the end, critical buckling load is equal to applied compressive load.

Figure 1.1: Topology optimization of a solid beam(all dimensions are in meters)

material removal (and profile of hollow regions) depends on the applied loading, the end conditions and the applied constraints. In this case, the constraint on buckling dominated.

In engineering components, plate or shell type structures are commonly used, e.g. wing panels, ribs, fuselage, cockpit of aircraft; bonnet and body of a car. Most of these structures are made of light material and "stiffened" using longitudinal and transverse members (spars, ribs,longerons,bulk heads). For a typical aircraft, a significant amount of the total structural weight is due to the stiffening components. Motivated by the simple example considered above, one can pose the following questions:

Is it possible to design the "optimal" stiffener configuration for a plate or shell-type structure?

In principle, topology optimization should lead to the best possible (minimum weight) configuration. Available topology optimisation procedure can be classified into the following groups:

a) Homogenisation based [14]

b) Soft kill/Hard kill [6]

c) Adaptivity based [3]

1.1.1 Homogenization based topology optimization

The domain is broken into a fine mesh of periodic cells(or subdomains) with the help of a very fine finite element mesh. Based on the current analysis of stress levels, due to an applied load, material is removed from a cell(element) whose Mises stress is below a lower threshold level. This may lead to a "porous" structure with filled and empty cells spread out. Getting a finite element solution of such fine mesh is impossible, and results may be useless due to spurious corners created in the domain(at vertices of hollow cells). Thus, the porous domain is homogenised and an average(smoothened) stress field is obtained, which is needed to propagate the

3

material removal(see [14]- [15] for details).

1.1.2 Soft kill/Hard kill

A fine mesh is made over the domain and material is removed(Hard kill) or replaced with a soft material(Soft kill) in elements with low average Mises stress(see [6]- [7] for details). The new material domain is again solved for till convergence.

1.1.3 Adaptivity based methods

The goal here is to accurately capture the low stress regions by refining the mesh adaptively in regions of low stress. This leads to very small sized elements at the boundaries of the low stress regions (i.e. stress below a given lower threshold). Material is then removed from the region, and the process is continued till convergence(see [3]- [5] for details).

The methods mentioned above suffer from the following drawbacks:

1. Spurious corners are created in the domains, where material is removed from an element. This leads to stress singularities, which causes the process to go back and forth without convergence. This is because the regions from which material gets removed demands material to be brought back at the next step.

2. Since average stress are taken, stress profiles are not very smooth.

3. The homogenization procedure can give stresses that are very different from the initial stress state(see [2]), and hence wrong design.

4. A fine mesh has to be resorted to in all cases, leading to heavy computational effort.

The flaws of the existing methods can be circumvented, if the following goals can be met:

1. Use of coarse mesh for the computation to reduce cost.

2. Get rid of spurious stress concentration induced due to the material removal strategy employed.

4

The current study is an attempt to systematically develop a procedure for topology optimization, which can meet the goals given above. The procedure given in this study utilizes the following tools:

1. Use a coarse mesh, with a good stress recovery algorithms, which should (in principle) give a better and smoothened stress field, as compared to the one obtained directly from the finite element solutions.

2. Capability to plot smooth contours of stress levels corresponding to a given threshold stress level.

3. Capability to remesh the new domains(with holes), with desired level of refinement at the interior boundaries.

Obviously, accurate representation of the pointwise stress is very important to ensure reliability of the design obtained. The recovered smoothened stress field can also be employed to get an estimate of the error in the approximation, which can be used for adaptive refinement of the finite element mesh obtained by remeshing.

1.2   ORGANISATION OF THE THESIS

The study in the thesis is organised as given below:

1. The first chapter deals with a discussion on the state-of-the-art and the goals of this study.

2. In chapter-2, a higher order plate theory(HSDT) is given. This plate theory will be used to study unsymmetric laminated plates.

3. In chapter-3, the finite element formulation corresponding to the HSDT model will be developed.

4. Chapter-4 deals with the a posteriori recovery of a smoothened stress field, from that obtained using the finite element method.

5. In chapter-5, the problem of an aluminium plate with an attached (underlying) steel plate is considered. The goal being to remove material from the steel plate, inorder to obtain a light weight design, appropriately stressed and safe plate design. The subsections in this chapter describes how contours are plotted

for the low stressed regions from the recovered smoothened stress field. These contours are drawn using a grid of "subelements" embeded in an element. The contours are polygonal in nature(obtained by connecting adjacent stress field points with a straight line). A spline based curve is fitted to the polygonal contours, to get smooth enclosed regions of low stress.

7. In the seventh chapter numerical problems are solved and results are shown.

8. Finally, chapter eight gives the scope of this work followed by discussion on the future scope.

Chapter 2

HIGHER ORDER PLATE THEORY

The relationship between the strains at any point within a laminate and the corresponding deformations are the functions of the assumed displacement fields. The displacement field and strain-displacement relationships are given below:

2.1 DEFINITION OF DISPLACEMENT FIELDS

The membrane-flexure coupling phenomenon exhibited by an unsymmetric laminate, necessiates the use of a displacement field containing both. The displacement field $\underline{V}(x, y, z) = [\, u(x, y, z), \, v(x, y, z), \, w(x, y, z)\,]$ is derived from the expanded Taylor's series in terms of thickness coordinate (z) is considered. This is given as, [1]

$$
\begin{aligned}
u(x, y, z) &= u_0(x, y) + z\theta_x(x, y) + z^2\phi_x(x, y) + z^3\psi_x(x, y); \\
v(x, y, z) &= v_0(x, y) + z\theta_y(x, y) + z^2\phi_y(x, y) + z^3\psi_y(x, y); \\
w(x, y, z) &= w_0(x, y)
\end{aligned} \tag{2.1}
$$

In the expansion (2.1), it is assumed that transverse normal strain ϵ_{zz} is zero. The linear strain-displacement relationships using small deformation theory can be written as follows:

$$\epsilon_{xx} = u_{0,x} + z\,\theta_{x,x} + z^2\,\phi_{x,x} + z^3\,\psi_{x,x};$$

$$\epsilon_{yy} = v_{0,y} + z\,\theta_{y,y} + z^2\,\phi_{y,y} + z^3\,\psi_{y,y};$$

$$\gamma_{xy} = u_{0,y} + z\,\theta_{x,y} + z^2\,\phi_{x,y} + z^3\,\psi_{x,y}$$

$$+v_{0,x} + z\,\theta_{y,x} + z^2\,\phi_{y,x} + z^3\,\psi_{y,x};$$

$$\gamma_{yz} = \theta_y + 2\,z\,\phi_y + 3\,z^2\,\psi_y + w_{0,y};$$

$$\gamma_{xz} = \theta_x + 2\,z\,\phi_x + 3\,z^2\,\psi_x + w_{0,x}$$

$$(2.2)$$

where comma (,) denotes the partial derivatives.
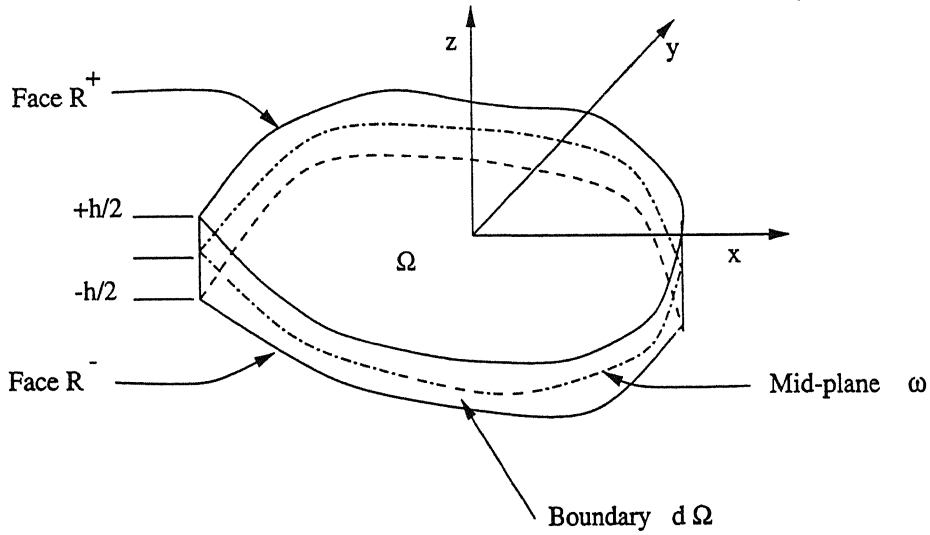
Figure 2.1: Representation of arbitrary three dimensional domain

The condition that the transverse shear stresses vanish on the plate's top and bottom faces (see Fig. 2.1) is equivalent to the requirement that the corresponding strains be zero on these surfaces, i.e.

$$\gamma_{yz}(x, y, \pm\tfrac{h}{2}) = \gamma_{xz}(x, y, \pm\tfrac{h}{2}) = 0$$

On introduction of the conditions as given above in the expressions for transverse

shear strains, the following relations are obtained.

$$\phi_x = \phi_y = 0 \qquad \text{and}$$

$$\psi_y = -\frac{4}{3h^2}(\theta_y + w_{0,y}) \ ; \qquad \psi_x = -\frac{4}{3h^2}(\theta_x + w_{0,x}) \tag{2.3}$$

The displacement field of Eq. (2.1) is modified by setting ϕ_x and ϕ_y to be zero according to conditions of Eq. (2.3). The resulting displacement field is written below:

$$u(x, y, z) = u_0(x, y) + z\,\theta_x(x, y) + z^3\,\psi_x(x, y);$$

$$v(x, y, z) = v_0(x, y) + z\,\theta_y(x, y) + z^3\,\psi_y(x, y); \tag{2.4}$$

$$w(x, y, z) = w_0(x, y)$$

In Eq. (2.4) u, v and w are the displacements along x, y and z directions respectively. u_0, v_0 and w_0 are the mid-plane displacements while θ_x, θ_y are rotations about y and x axes, respectively. Whereas, ψ_x and ψ_y are higher order terms in the Taylor's series expansion and are also defined at mid-plane. Thus, the generalised displacement vector $\{\delta\}$ of the mid-surface contains seven degrees of freedom (DOF) and is given by:

$$\{\delta\} = \{u_0, v_0, w_0, \theta_x, \theta_y, \psi_x, \psi_y\}^T.$$

Corresponding strain-displacement relationship becomes:

$$\epsilon_{xx} = u_{0,x} + z\,\theta_{x,x} + z^3\,\psi_{x,x};$$

$$\epsilon_{yy} = v_{0,y} + z\,\theta_{y,y} + z^3\,\psi_{y,y};$$

$$\gamma_{xy} = u_{0,y} + z\,\theta_{x,y} + z^3\,\psi_{x,y}$$

$$\qquad + v_{0,x} + z\,\theta_{y,x} + z^3\,\psi_{y,x}; \tag{2.5}$$

$$\gamma_{yz} = \theta_y + 3\,z^2\,\psi_y + w_{0,y};$$

$$\gamma_{xz} = \theta_x + 3\,z^2\,\psi_x + w_{0,x}$$

2.2 LAMINATE CONSTITUTIVE EQUATIONS

A unidirectional fibre reinforced lamina is treated as an orthotropic material whose material symmetry planes are parallel and transverse to the fiber direction.
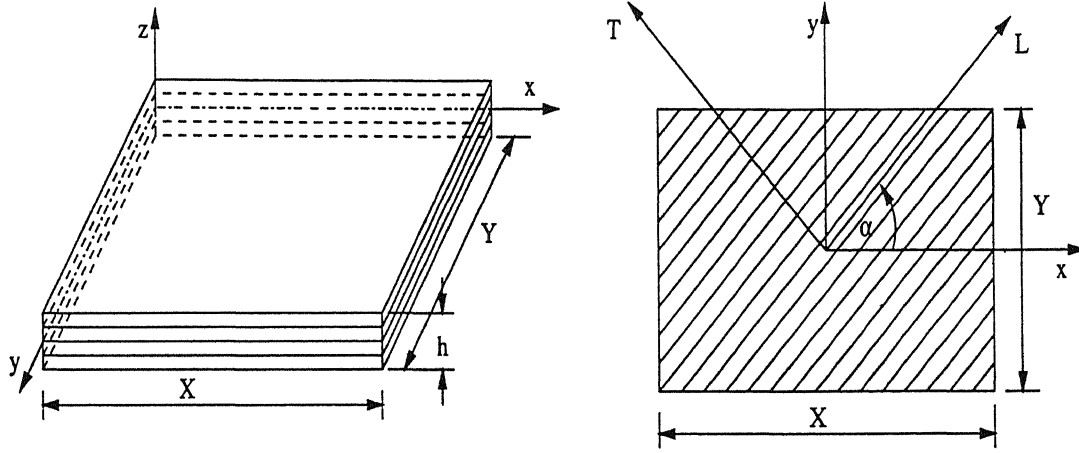
Figure 2.2: Co-ordinate axes in lamina

Following fig. (2.2) the material co-ordinates axes L and T are defined parallel and perpendicular to the fibre direction respectively, while global co-ordinates are x and y. The angle between global co-ordinate axis x and fibre direction, material co-ordinate axis L, is α and is known as the orientation angle. As a sign convention anticlockwise angle is taken as positive.

Generalized Hooke's law

In the formulation of lamina constitutive equation following two assumptions are made.

1. The lamina is a continuum.

2. It behaves as a linearly elastic material.

Further, at the micro-level the following assumptions are made about the material:

1. Perfect bonding between fibres and matrix exists.

2. Fibres are parallel and uniformly distributed throughout.

10

3. The matrix is free of voids or micro cracks and initially in a stress free state.

4. Both fibres and matrix are isotropic and obey Hook's law.

Stress-strain relations for the lth lamina in the material coordinate axis, whose fibers are oriented at an angle α with reference to the x axis is given as ([?], [?]):

$$\left\{ \sigma_i \right\}_l = [\bar{Q}_{ij}]_l \left\{ \epsilon_j \right\}_l \qquad (2.6)$$

where $\{\sigma_i\}$ is the vector of stress components, $[\bar{Q}_{ij}]$ is the stiffness matrix, and $\{\epsilon_j\}$ are the engineering strain components, for the lth lamina.

The stresses and strains in the x, y and z directions are obtained by transformation relations given in equation (2.6). The transformed stress strain relations for the lth lamina are given as:

$$\left\{ \begin{array}{c} \sigma_x \\ \sigma_y \\ \tau_{xy} \\ \tau_{yz} \\ \tau_{xz} \end{array} \right\}_l = \left[\begin{array}{ccccc} \bar{Q}_{11} & \bar{Q}_{12} & \bar{Q}_{16} & 0 & 0 \\ \bar{Q}_{21} & \bar{Q}_{22} & \bar{Q}_{26} & 0 & 0 \\ \bar{Q}_{16} & \bar{Q}_{26} & \bar{Q}_{66} & 0 & 0 \\ 0 & 0 & 0 & \bar{Q}_{44} & \bar{Q}_{45} \\ 0 & 0 & 0 & \bar{Q}_{45} & \bar{Q}_{55} \end{array} \right]_l \left\{ \begin{array}{c} \epsilon_x \\ \epsilon_y \\ \gamma_{xy} \\ \gamma_{yz} \\ \gamma_{xz} \end{array} \right\}_l \qquad (2.7)$$

Using the above lamina constitutive equations and integrating the stresses over the laminate thickness, the stress resultants in terms of inplane forces, moments and shear forces per unit length, for a laminate with NL laminae are,

$$\left\{ \begin{array}{c} \{N\} \\ \{M\} \\ \{M^*\} \\ \{Q\} \\ \{Q^*\} \end{array} \right\} = \left[\begin{array}{ccc} [D_m] & [D_c] & 0 \\ [D_c]^T & [D_b] & 0 \\ 0 & 0 & [D_s] \end{array} \right] \left\{ \begin{array}{c} \{\epsilon_0\} \\ \{\kappa\} \\ \{\kappa^*\} \\ \{\nu\} \\ \{\nu^*\} \end{array} \right\} \qquad (2.8)$$

where $\{\epsilon_0\}$ are the mid-plane strains, $\{\kappa\}$ are the mid-surface curvatures and $\{\kappa^*\}$, $\{\nu\}$, $\{\nu^*\}$ are higher order terms and

$$\{N\}^T = (N_x, N_y, N_{xy}) = \sum_{l=1}^{NL} \int_{z_l}^{z_{l-1}} (\sigma_x, \sigma_y, \sigma_{xy})^l \quad dz; \qquad (2.9)$$

11

$$\{\mathbf{M}\}^{\mathbf{T}} = (M_x, M_y, M_{xy}) = \sum_{l=1}^{NL} \int_{z_l}^{z_{l-1}} (\sigma_x, \sigma_y, \sigma_{xy})^l \ z \ dz; \tag{2.10}$$

$$\{\mathbf{M}^*\}^{\mathbf{T}} = (M_x^*, M_y^*, M_{xy}^*) = \sum_{l=1}^{NL} \int_{z_l}^{z_{l-1}} (\sigma_x, \sigma_y, \sigma_{xy})^l \ z^3 \ dz; \tag{2.11}$$

$$\{\mathbf{Q}\}^{\mathbf{T}} = (Q_x, Q_y) = \sum_{l=1}^{NL} \int_{z_l}^{z_{l-1}} (\tau_{xz}, \tau_{yz})^l \ dz; \tag{2.12}$$

$$\{\mathbf{Q}^*\}^{\mathbf{T}} = (Q_x^*, Q_y^*) = \sum_{l=1}^{NL} \int_{z_l}^{z_{l-1}} (\tau_{xz}, \tau_{yz})^l \ z^2 \ dz. \tag{2.13}$$

Here, z_i are the z coordinates corresponding to the laminae interfaces as shown in Fig 2.3.

The other terms and following rigidity matrices are given in Appendix A.
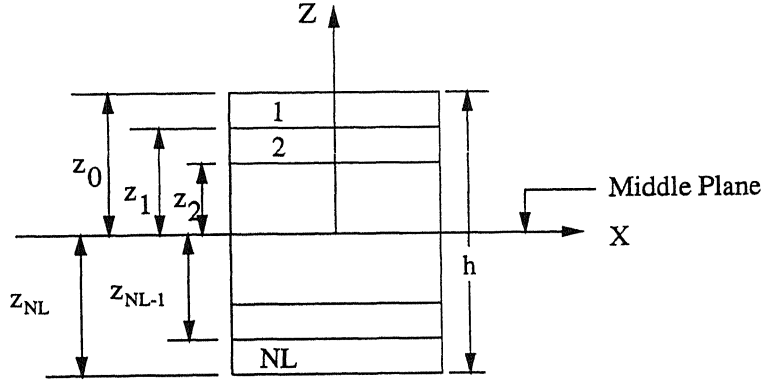
Figure 2.3: Geometry of multilayer laminate

Thus, with the assumed displacement model, the various rigidity matrices derived are:

$[D_m]$ = Membrane; $[D_c]$ = Membrane-flexure coupling.

$[D_b]$ = Flexure; $[D_s]$ = Shear.

The set of rigidity matrices $[D_m], [D_c], [D_b]$ and $[D_s]$ are used in forming overall rigidity matrix $[D_r]$ for the laminate.

Chapter 3

FINITE ELEMENT FORMULATION

Triangular elements are used for finite element discretisation and hierarchic shape functions of order p ($p \leq 4$) are used for finite element approximation. The mesh generation is done using automatic mesh generator and a mesh generated over the plate domain is shown in fig. (3.1).
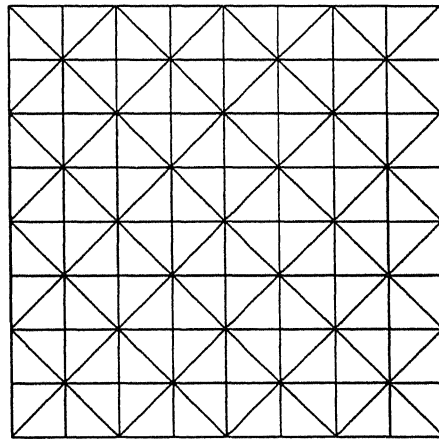
Figure 3.1: Mesh generated over a square domain

3.1 DEFINITIONS

Let $\{V\}$ be the displacement vector defined as:

$$\{V\} = \left\{ \begin{array}{c} u \\ v \\ w \end{array} \right\} \tag{3.1}$$

Let the stress and strain vectors corresponding to $\{V\}$ be $\{\sigma\}$ and $\{\epsilon\}$ which can be defined as:

$$\{\sigma\} = \left\{ \begin{array}{c} \sigma_x \\ \sigma_y \\ \tau_{xy} \\ \tau_{yz} \\ \tau_{xz} \end{array} \right\} \qquad \{\epsilon\} = \left\{ \begin{array}{c} \epsilon_x \\ \epsilon_y \\ \gamma_{xy} \\ \gamma_{yz} \\ \gamma_{xz} \end{array} \right\} \tag{3.2}$$

From the generalized Hooke's law which relates stress components to the respective strain components in global coordinate system

$$[\sigma] = [\bar{Q}] \{\epsilon\} \tag{3.3}$$

where material stiffness matrix $[\bar{Q}]$ for orthotropic material is as given in Eq. (2.7) for each lamina.

In any elastic body, linear strain-displacement relationships using small deformation theory is given in Eq. (2.5).

The above relations in the matrix form can be expressed as:

$$\{\epsilon\} = [\bar{D}] \{V\} \tag{3.4}$$

where $[\bar{D}]$ is a differential operator in terms of global coordinates such that

$$[\bar{D}] = \begin{bmatrix} \frac{\partial}{\partial x} & 0 & 0 \\ 0 & \frac{\partial}{\partial y} & 0 \\ \frac{\partial}{\partial y} & \frac{\partial}{\partial x} & 0 \\ 0 & \frac{\partial}{\partial z} & \frac{\partial}{\partial y} \\ \frac{\partial}{\partial z} & 0 & \frac{\partial}{\partial x} \end{bmatrix} \tag{3.5}$$

14

The components of displacement can be written in terms of the seven unknown in-plane functions, which can be written as:

$$\{\delta\}^T = \{u_0, v_0, w_0, \theta_x, \theta_y, \psi_x, \psi_y\}$$

The displacement vector is written in matrix form as

$$\{V\} = [\Phi] \{\delta\} \tag{3.6}$$

where

$$[\Phi] = \begin{bmatrix} 1 & 0 & 0 & z & 0 & z^3 & 0 \\ 0 & 1 & 0 & 0 & z & 0 & z^3 \\ 0 & 0 & 1 & 0 & 0 & 0 & 0 \end{bmatrix} \tag{3.7}$$

In the finite element approximation the functions u_0, v_0, ... etc are approximated using n shape functions per element.

$$\begin{Bmatrix} u_0 \\ v_0 \\ w_0 \\ \theta_x \\ \theta_y \\ \psi_x \\ \psi_y \end{Bmatrix} = \sum_{i=1}^{n} N_i \begin{Bmatrix} u_{0i} \\ v_{0i} \\ w_{0i} \\ \theta_{xi} \\ \theta_{yi} \\ \psi_{xi} \\ \psi_{yi} \end{Bmatrix} \tag{3.8}$$

$$\{\delta\} = \sum_{i=1}^{n} N_i \{\delta_i\} \tag{3.9}$$

where, $n = (p+1)(p+2)/2$ is the number of independent coefficients in an element, p is the approximation order, N_i is the ith shape function associated with i^{th} independent coefficient in terms of normalised coordinates ξ and η and $\{\delta_i\}$ is the generalized displacement vector corresponding to i^{th} independent coefficient of an element.

Remark: When Lagrangian shape functions are used, the independent coefficients correspond to physical nodes.

15

Hence displacement vector can be written as

$$\{V\} = [\Phi]\,[N]\,\{d\} \tag{3.10}$$

where $\{d\}^T = \{\{\delta_1\}^T, \{\delta_2\}^T, ...\{\delta_n\}^T\}$ and $[N]$ is a matrix in terms of n inplane hierarchic shape functions given in *Appendix B*.

Hence, the strain vector can be written as

$$\{\epsilon\} = ([\bar{D}]\,[\Phi]\,[N])\,\{d\} \tag{3.11}$$

and the stress vector

$$\{\sigma\} = [\bar{Q}]\,([\bar{D}]\,[\Phi]\,[N])\,\{d\} \tag{3.12}$$

3.2 FINITE ELEMENT FORMULATION USING ENERGY PRINCIPLE

The total potential for the plate is given by

$$\Pi\,(\delta) = \sum_{e=1}^{N} \pi^e\,(\delta), \tag{3.13}$$

where π^e is the total potential of the non-intersecting (but adjacent) sub-domians e which are part of the domain (N sub-domains are considered here). The total potential can be expressed in terms of internal strain energy $U^{(e)}$ and external work done $W^{(e)}$, as follows:

$$\pi^e\,(\delta) = U^{(e)} - W^{(e)}. \tag{3.14}$$

Strain energy of the laminate can expressed as follows:

$$U^{(e)} = \frac{1}{2}\int_{V^{(e)}}\{\epsilon\}^T\,[\sigma]\,dV^{(e)} \tag{3.15}$$

Work done by the applied external transverse load is,

$$\begin{aligned}
W^{(e)} &= \int_{A^{(e)}}\{V\}^T_{z=\pm\frac{h}{2}}\,f\,dA^{(e)} \\
&= \int_{R^{+(e)}} w_0\,f^+\,dA^{(e)} + \int_{R^{-(e)}} w_0\,f^-\,dA^{(e)}
\end{aligned} \tag{3.16}$$

16

where f^+ is the transverse load on the top face R^+ and f^- is the transverse load on the top face R^-.

The exact solution $\underline{u}_{ex}$ to this problem is the minimization of the total potential Π. This can be obtained as:

$$\delta^{(1)} \Pi = 0,$$

which is also the *Virtual Work Formulation* of the problem in terms of the components of δ. From this, the seven coupled equilibrium equations in terms of the components of δ can be obtained. This leads to generalised finite element formulation:

$$[K]\{d\} = \{F\} \tag{3.17}$$

where $[K]$ is the stiffness matrix and $\{F\}$ is load vector.

In the next section, we are going to employ the virtual work formulation to derive the finite element formulation of this problem.

3.3 COMPUTATION OF ELEMENT STIFFNESS MATRIX

The stiffness matrix corresponding to assumed deformation state of an element can be defined by expressing the internal strain energy in terms of unknown nodal displacements. In the formulation of unsymmetric laminates the membrane, the flexure,membrane-flexure coupling and shear strains contribute to strain energy. The set of Eq. (2.5) can be used along with Eq. (3.12), (3.15) to express these strains in terms of nodal displacements.

The internal strain energy of an element (given by area A^e) can be determined as:

$$
\begin{aligned}
U^e = \tfrac{1}{2} \int_{A^e} \big(& \{d\}^T \left([B_m]^T [D_m] [B_m] \right) \{d\} + \{d\}^T \left([B_b]^T [D_b] [B_b] \right) \{d\} \\
& + \{d\}^T \left([B_s]^T [D_s] [B_s] \right) \{d\} + \{d\}^T \left([B_m]^T [D_c] [B_b] \right) \{d\} \\
& + \{d\}^T \left([B_b]^T [D_c] [B_m] \right) \{d\} \big) \, dA
\end{aligned}
\tag{3.18}
$$

17

Here the first term on the right-hand side of Eq. (3.18) is the in-plane contribution, the second and third terms are out-of-plane bending and through-thickness shearing contributions, respectively. The last two terms are contributions from coupling between in-plane and out-of-plane actions.

The strain energy expression can be written in a concise form as:

$$U^{(e)} = \frac{1}{2} \{d^e\}^T [K^e] \{d^e\} \tag{3.19}$$

where $[K^e]$ is the stiffness matrix and $\{d^e\}$ are the coefficients corresponding to the finite element solution in an element e. All the terms in equation (3.18) are evaluated individually and then summed to yield $[K^e]$.

It is given by:

$$[K^e] = \int_{A^e} [\ ([B_m]^T [D_m] [B_m]) + ([B_b]^T [D_b] [B_b]) + ([B_s]^T [D_s] [B_s]) \\ + ([B_m]^T [D_c] [B_b]) + ([B_b]^T [D_c] [B_m])\ ]\ dA \tag{3.20}$$

The numerical integration is carried out to get element stiffness matrix.
The matrices $[B_m], [B_b]$ and $[B_c]$ and vector $\{d\}$ are given in Appendix B.

3.4 COMPUTATION OF ELEMENT LOAD VECTOR

For the extension and/or bending problems of laminated plates, the applied external forces may consist of following cases of loading:

1. Uniformly distributed load acting over the element in the z-direction on top or bottom bounding planes of the plate.

2. Sinusoidal distributed load acting over the element in the z-direction on top or bottom bounding planes of the plate.

3. Traction load acting along the edges in the x or y-direction .

The total external work done by these forces on an element can be expressed as

18

follows:

$$W^e = \{d\}^T \int_S ([\Phi]\,[N])^T \{T_r\}\, dS \qquad (3.21)$$

or

$$W^e = \{d\}^T \{F^e\} \qquad (3.22)$$

where $\{F^e\}$ is the element load vector, and the traction vector is given as:

$$\{T_r\} = \left\{ \begin{array}{c} T_x \\ T_y \\ T_z \end{array} \right\} \qquad (3.23)$$

Transverse loading, T_z can be sinusoidal as $T_z = P_c \sin(\frac{m\pi x}{X}) \sin(\frac{n\pi y}{Y})$ or uniform pressure $T_z = P_0$. T_x, T_y can be uniform inplane tractions along x and y, repectively.

3.5   GEOMETRIC APPROXIMATION

3.5.1   STRAIGHT EDGE ELEMENTS

The geometry is expressed in terms of the shape functions as:

$$\left\{ \begin{array}{c} x \\ y \end{array} \right\} = \sum_{i=1}^{3} N_i \left\{ \begin{array}{c} x_i \\ y_i \end{array} \right\} \qquad (3.24)$$

where, $\left\{ \begin{array}{c} x_i \\ y_i \end{array} \right\}$ are the coordinates of the ith node of the element, and N_i are the linear shape functions of the element.

LINEAR MAPPING:

Linear mapping in general is used when all sides of mapped elements are straight lines(see Fig. 3.2). Consider the mapping of variables from x,y to ξ, η such that $\{x, y \in A\}$ on substitution of N_i these can be written in the matrix form as

$$\left\{ \begin{array}{c} x - x_1 \\ y - y_1 \end{array} \right\} = \left[\begin{array}{cc} x_2 - x_1 & x_3 - x_1 \\ y_2 - y_1 & y_3 - y_1 \end{array} \right] \left\{ \begin{array}{c} \xi \\ \eta \end{array} \right\} \qquad (3.25)$$
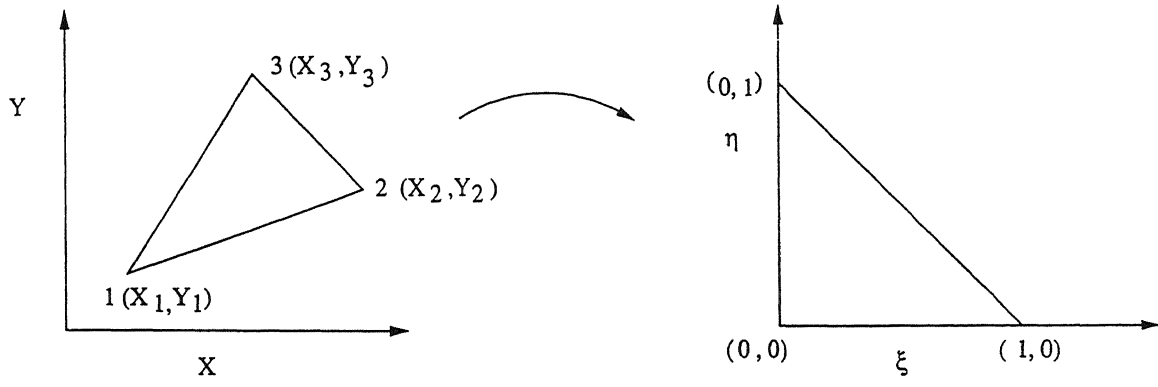
Figure 3.2: Linear mapping in two dimension

Clearly,

$$\frac{\partial x}{\partial \xi} = x_2 - x_1 \qquad \frac{\partial x}{\partial \eta} = x_3 - x_1$$
$$\frac{\partial y}{\partial \xi} = y_2 - y_1 \qquad \frac{\partial y}{\partial \eta} = y_3 - y_1 \qquad (3.26)$$

On inverting the matrix it is easy to see that

$$\left\{ \begin{array}{c} \xi \\ \eta \end{array} \right\} = \frac{1}{\Delta} \left[\begin{array}{cc} (y_3 - y_1) & -(x_3 - x_1) \\ -(y_2 - y_1) & (x_2 - x_1) \end{array} \right] \left\{ \begin{array}{c} x - x_1 \\ y - y_1 \end{array} \right\} \qquad (3.27)$$

where, $\qquad \Delta = (x_2 - x_1)(y_3 - y_1) - (x_3 - x_1)(y_2 - y_1)$

Hence,

$$\frac{\partial \xi}{\partial x} = \frac{y_3 - y_1}{\Delta} \qquad \frac{\partial \xi}{\partial y} = -\frac{x_3 - x_1}{\Delta}$$
$$\frac{\partial \eta}{\partial x} = -\frac{y_2 - y_1}{\Delta} \qquad \frac{\partial \eta}{\partial y} = \frac{x_2 - x_1}{\Delta} \qquad (3.28)$$

Transforming $dxdy$ **into** $d\xi d\eta$:

Let the differential area $dxdy$ is formed through vectors $\hat{dx}$ and $\hat{dy}$ with magnitude dA and direction normal to the elemental area is $\hat{k}$

$$dA = dx\, dy = [\hat{dx} \times \hat{dy}] \cdot \hat{k} \qquad (3.29)$$

$$dx\, dy = [\, (\, \tfrac{\partial x}{\partial \xi}\, d\xi\, \hat{i} + \tfrac{\partial x}{\partial \eta}\, d\eta\, \hat{j}\,) \times (\, \tfrac{\partial y}{\partial \xi}\, d\xi\, \hat{i} + \tfrac{\partial y}{\partial \eta}\, d\eta\, \hat{j}\,)\,]\cdot \hat{k}$$
$$= [\, \tfrac{\partial x}{\partial \xi} \cdot \tfrac{\partial y}{\partial \eta} - \tfrac{\partial x}{\partial \eta} \cdot \tfrac{\partial y}{\partial \xi}\,]\, d\xi\, d\eta \qquad (3.30)$$
$$= |J|\, d\xi\, d\eta$$

20

or the Jacobian matrix is given by

$$J = \begin{bmatrix} \frac{\partial x}{\partial \xi} & \frac{\partial y}{\partial \xi} \\ \frac{\partial x}{\partial \eta} & \frac{\partial y}{\partial \eta} \end{bmatrix} \tag{3.31}$$

Substituting from equation (3.5)

$$|J| = (x_2 - x_1)(y_3 - y_1) - (x_3 - x_1)(y_2 - y_1) \tag{3.32}$$

Hence $\int_e f(x, y)\, dx\, dy$ may be written as

$$\int_e f(x, y)\, dx\, dy = \int_{e_m} \hat{f}(\xi, \eta)\, d\xi\, d\eta \tag{3.33}$$

such that $\hat{f}(\xi, \eta)\, d\xi\, d\eta = |J|\, f(x(\xi, \eta), y(\xi, \eta))$.

Numerical Integration:

To compute $\int_{A_m} \hat{f}(\xi, \eta)\, d\xi\, d\eta$ *Gaussian quadrature* for two-dimentional integrals is used through which

$$\int_{A_m} \hat{f}(\xi, \eta)\, d\xi\, d\eta \approx \sum_{i=1}^{n} \hat{f}(\xi_i, \eta_i)\, w_i\, |J| \tag{3.34}$$

where, n is the number of quadrature points, w_i is the weight at quadrature point (ξ_i, η_i) and the Jacobian $|J|$ is the area of the element e.

Order of numerical integration is greater than or equal to $(p + 1)/2$ where, p is the order of the integrand.

Shape Function Derivatives:

Shape functions are defined in the master element i.e. $N_i = N_i(\xi, \eta)$. Its derivatives with respect to x and y can be given as

$$\begin{aligned} N_{i,x} &= \frac{\partial N_i}{\partial \xi} \cdot \frac{\partial \xi}{\partial x} + \frac{\partial N_i}{\partial \eta} \cdot \frac{\partial \eta}{\partial x} \\ N_{i,y} &= \frac{\partial N_i}{\partial \xi} \cdot \frac{\partial \xi}{\partial y} + \frac{\partial N_i}{\partial \eta} \cdot \frac{\partial \eta}{\partial y} \end{aligned} \tag{3.35}$$

Since shape functions are defined in terms of normalised coordinates ξ and η the terms $\frac{\partial N_i}{\partial \xi}$ and $\frac{\partial N_i}{\partial \eta}$ can be evaluated at any point in the domain.

21

Chapter 4

RECOVERY OF SMOOTHENED STRESS FIELD

4.1 RECOVERY OF STRAINS

Recovered strain-field over an element are constructed using *patch-recovery* technique [13]. In this recovered strains are obtained using minimization of energy norm of error over the patch(see Fig. 4.1) around an element J. Thus, the problem can be posed as:

find $\underline{\varepsilon}^*$ such that

$$J = \frac{1}{2} \int_{A_{patch}} \int_{z=-\frac{h}{2}}^{\frac{h}{2}} \left(\underline{\varepsilon}_{FE} - \underline{\varepsilon}^* \right) \cdot \bar{Q} \left(\underline{\varepsilon}_{FE} - \underline{\varepsilon}^* \right) \, dz \, dA \tag{4.1}$$

is minimized. Here $\underline{\varepsilon}^*$ and $\underline{\varepsilon}_{FE}$ are recovered and finite element strain vectors and $\bar{Q}$ is material stiffness matrix, respectively.

The finite element strains and material stiffeness properties are already available over the patch. The recovered strains are constructed using the same mathematical
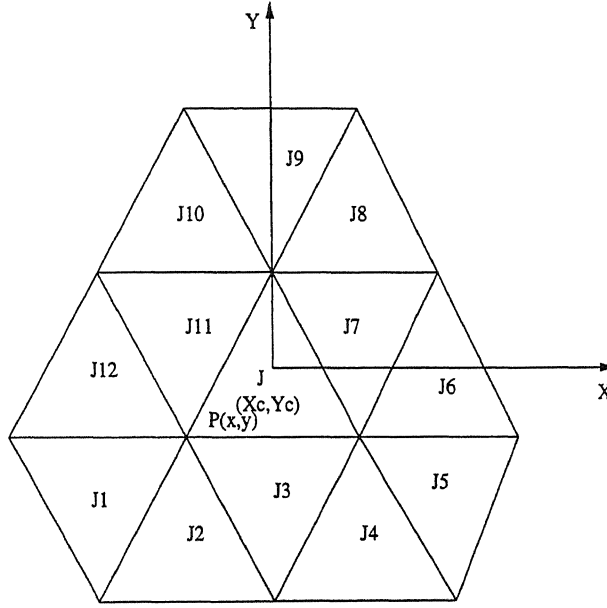
Figure 4.1: Patch over element J

form as that of the exact solution of the model i.e.

$$\epsilon^{*}_{xx} = \epsilon^{*0}_{xx} + z\,\epsilon^{*1}_{xx} + z^3\,\epsilon^{*2}_{xx}$$

$$\epsilon^{*}_{yy} = \epsilon^{*0}_{yy} + z\,\epsilon^{*1}_{yy} + z^3\,\epsilon^{*2}_{yy}$$

$$\epsilon^{*}_{xy} = \epsilon^{*0}_{xy} + z\,\epsilon^{*1}_{xy} + z^3\,\epsilon^{*2}_{xy} \tag{4.2}$$

$$\gamma^{*}_{yz} = \gamma^{*0}_{yz} + z^2\,\gamma^{*1}_{yz}$$

$$\gamma^{*}_{xz} = \gamma^{*0}_{xz} + z^2\,\gamma^{*1}_{xz}$$

In-plane strains of the strain tensor are approximated by p^{th} order polynomial and are given by

$$\epsilon^{*0}_{xx} = \sum_{i=1}^{(p+1)(p+2)/2} e^{*0}_{xx,i}\,q_i \tag{4.3}$$

Similarly, the strain components $\epsilon^{*1}_{xx}, \epsilon^{*2}_{xx}, \epsilon^{*0}_{yy}, \epsilon^{*1}_{yy}, \epsilon^{*2}_{yy}, \epsilon^{*0}_{xy}, \epsilon^{*1}_{xy}, \epsilon^{*2}_{xy}$ can be approximated as above(eqn. 4.3). Whereas, the transverse shear strains of the strain tensor are approximated by $(p+1)^{th}$ order polynomial and are given by

$$\gamma^{*0}_{yz} = \sum_{i=1}^{(p+2)(p+3)/2} e^{*0}_{yz,i}\,q_i \tag{4.4}$$

Similarly, $\gamma^{*1}_{yz}, \gamma^{*0}_{xz}, \gamma^{*1}_{xz}$ strain components can be approximated as above(eqn. 4.4). The minimization problem 4.1 can be restated in terms of the unknown coefficients,

23

$e^{*0}_{xx,i}, e^{*1}_{xx,i}, \ e^{*2}_{xx,i}, e^{*0}_{yy,i}, e^{*1}_{yy,i}, \ e^{*2}_{yy,i}, e^{*0}_{xy,i}, e^{*1}_{xy,i}, \ e^{*2}_{xy,i}, \gamma^{*0}_{yz,i}, \ \gamma^{*1}_{yz,i}, \gamma^{*2}_{yz,i}, \ \gamma^{*0}_{xz,i}, \gamma^{*1}_{xz,i},$

$\gamma^{*2}_{xz,i}.$ This leads to a matrix problem over each patch. The monomials(shape functions) q_i used in the representation 4.3,4.4 are given by

$$
\begin{array}{lll}
q_1 = 1 & q_2 = \hat{x} & q_3 = \hat{y} \\[4pt]
q_4 = \hat{x}^2 & q_5 = \hat{x}\hat{y} & q_6 = \hat{y}^2 \\[4pt]
q_7 = \hat{x}^3 & q_8 = \hat{x}^2\hat{y} & q_9 = \hat{x}\hat{y}^2 \\[4pt]
q_{10} = \hat{y}^3 & q_{11} = \hat{x}^4 & q_{12} = \hat{x}^3\hat{y} \\[4pt]
q_{13} = \hat{x}^2\hat{y}^2 & q_{14} = \hat{x}\hat{y}^3 & q_{15} = \hat{y}^4 \\[4pt]
q_{16} = \hat{x}^5 & q_{17} = \hat{x}^4\hat{y} & q_{18} = \hat{x}^3\hat{y}^2 \\[4pt]
q_{19} = \hat{x}^2\hat{y}^3 & q_{20} = \hat{x}\hat{y}^4 & q_{21} = \hat{y}^5
\end{array}
\tag{4.5}
$$

where

$$
\left\{ \begin{array}{c} \hat{x} \\ \hat{y} \end{array} \right\} = \left\{ \begin{array}{c} X_c - x \\ Y_c - y \end{array} \right\}
\tag{4.6}
$$

Here (X_c, Y_c) represents centroid of the element J and $P(x, y)$ is any point in the patch. Solution of the matrix problem over a patch gives the coefficients corresponding to the expansion over the patch. The components of the recovered strain field are then represented in terms of lagrangian shape function (of the same order as that used for the polynomial fitting). Thus, we obtain "nodal" values of the recovered strain components, for any element J (see Fig. 4.2).

$$
\epsilon^{*0}_{xx}(x_j, y_j) = \sum_{i=1}^{(p+1)(p+2)/2} e^{*0}_{xx,i} \ q_i(x_j, y_j)
\tag{4.7}
$$

$$
\epsilon^{*0}_{xx}(x, y) = \sum_{j=1}^{NN} \epsilon^{*0}_{xx}(x_j, y_j) \ N_j^l
\tag{4.8}
$$

Here N_j^l represents lagrange shape function associated with j^{th} node in terms of normalised coordinates ξ and η ,NN represents number of nodes, $q_i(x_j, y_j)$ represents monomials at j^{th} nodal coordinates, $\epsilon^{*0}_{xx}(x_j, y_j)$ represents the recovered strain components at j^{th} nodal coordinates. Similarly all the recovered strain components are obtained for all the nodes in the Jth element. This process is carried out through all the elements and recovered strain components are obtained for all the element nodes.

24
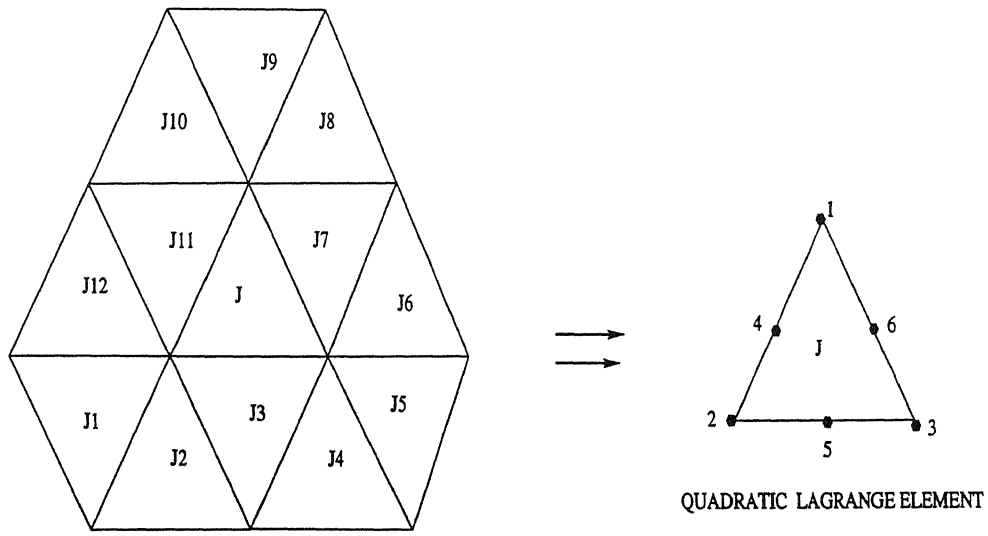
Figure 4.2: J^{th} element in the patch is represented in terms of lagrange quadratic element

4.1.1 Special Case: Adjoining dissimilar material domains
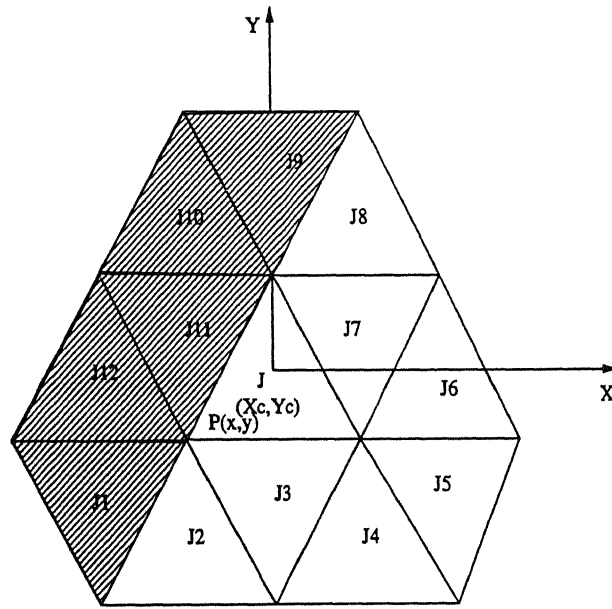
Figure 4.3: Patch over element J with adjoining dissimilar material domains

Consider a patch as shown in figure 4.3, Here the shaded elements have different material properties as compared with unshaded elements. In this case, while recovering strains over the element J , the elements with different material properties

when compared with J^{th} element will not be considered. For the figure shown while recovering strains for element J in patch information the elements $J9, J10, J11, J12$ and $J1$ will not be considered, since it is known that when material properties changes then strains are discontinous at the boundaries where material properties changes.

4.2 SMOOTHENED STRESS FIELD

The recovered smoothened strain components are obtained by averaging recovered strain components over each node to get single value per node. This ensures continuity of strains at element boundaries. For example, figure 4.4(A) shows a patch of quadratic Lagrange elements, It has 6 nodes per element. Here recovered strain components for each element nodes are found separately by constructing a patch over each element. Because of this, the nodal strains in element A and in element B are not continous at their interface, thus you can visualize this effect as if the two elements are getting seperated by a marginal distance (see figure 4.4(B)(i)). In order to get continuity at element interface(see figure 4.4(B)(ii)), the recovered strain components are averaged at the common nodes, which the two elements shares. i.e., the recovered strain components of the nodes 3 and 8 in elements A and B are taken and their values are replaced by its average value respectively. Look at the node 13, it is shared by elements A,B,C,D,E,F,G and H so the recovered strain components of the node 13 in all the elements are taken and replaced by its average value. This process is repeated for each and every node to ensure continuity of strains over the element boundaries. Then the recovered strains are obtained at desired laminate thickness using the relations given in equation 4.2 .

The plate model that is considered guarantees continuity of inplane stresses and strains,thus the inplane stresses are obtained through laminate constitutive equations which are given in equation (2.7) , but in out of plane direction the plate model guarentees only strain continuity and not stress continuity. Hence the

26
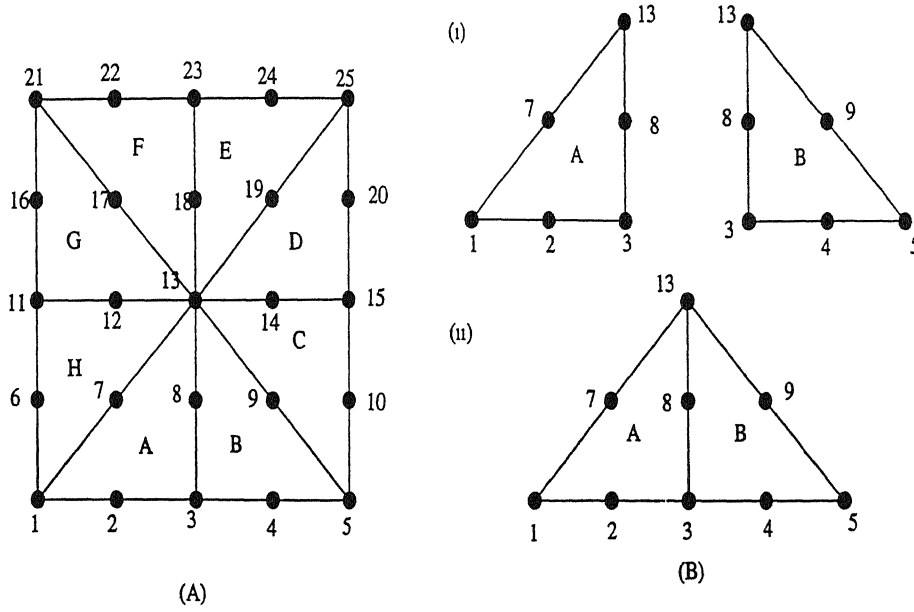
Figure 4.4: Sharing of nodes over element patches

transverse stress field are obtained from the equilibrium equations.

To make engineering decisions one should guarantee that the finite element stresses that are obtained are sufficiently close to exact solution of the mathematical model considered. To check the accuracy we should do error estimation to validate our results. If error is high, we have to go for adaptive mesh generation to reduce the error and to correct our solution to come closer to exact solution. Since we are in the nascent stage of this study. we are proceeding with our recovered smoothened stresses without doing any adaptive mesh generation using error estimation procedures. We are in a step prior to error estimation and in near future those modules will be added.

Chapter 5

THE PROBLEM OF STIFFENER DESIGN

Light weight vehicles(e.g. aeroplanes,light transport vehicles) have the outer structures made of aluminium alloys with suitable stiffeners to provide stiffness under bending and on shear loads. With this as a motivation, we consider the idealized sample stiffened plate configuration defined below.

5.1 STIFFENED PLATE

The stiffened laminated plate is taken as shown in Fig.5.1. The skin(top lamina) is taken to be made of aluminium alloy and the bottom stiffener is taken to be made of steel alloy. The goal being to remove material iteratively from the minimally stressed regions in stiffener such that the final configuration of the stiffened plate is an appropriately stressed minimum weight safe structure. The safe structure should satisfy the following conditions:

1. The plate considered should not yield.
2. The plate should not buckle.
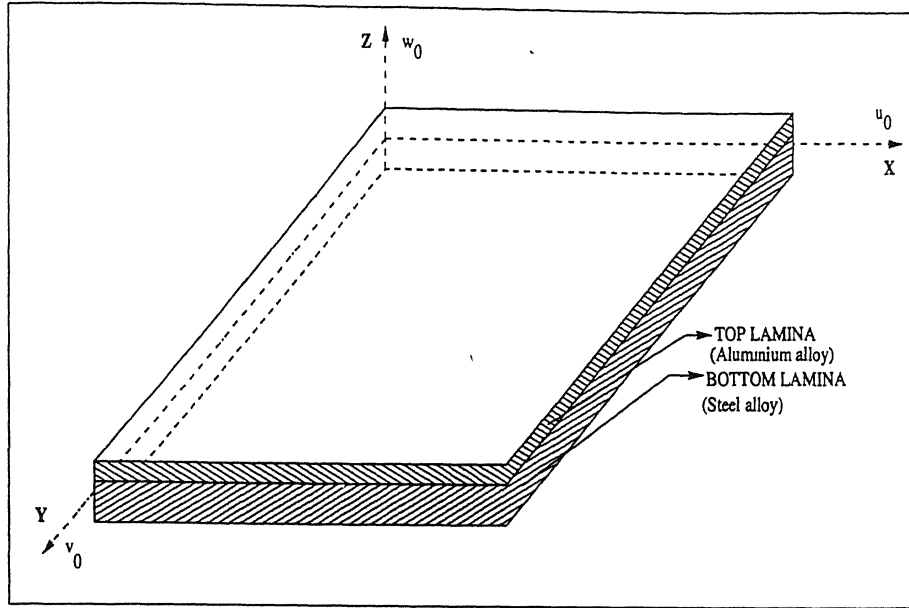
Figure 5.1: Initial shape of stiffened plate

3. The plate should not fail in vibrations.

As an initial step in our study we are considering only the first condition. The procedure for optimizing stiffener topology is given below.

5.2 PROCEDURE OF STIFFENER TOPOLOGY OPTIMIZAION

A flowchart is given in figure 5.2 which shows the main stages in the stiffener topology optimization algorithm embedded in our program. User-defined parameters control the execution of the program and evolution of the structure. The details of the evolution are as given below.

The initial structure is completely defined by the finite element mesh and this is read in together with applied loading and restraints. The finite element problem
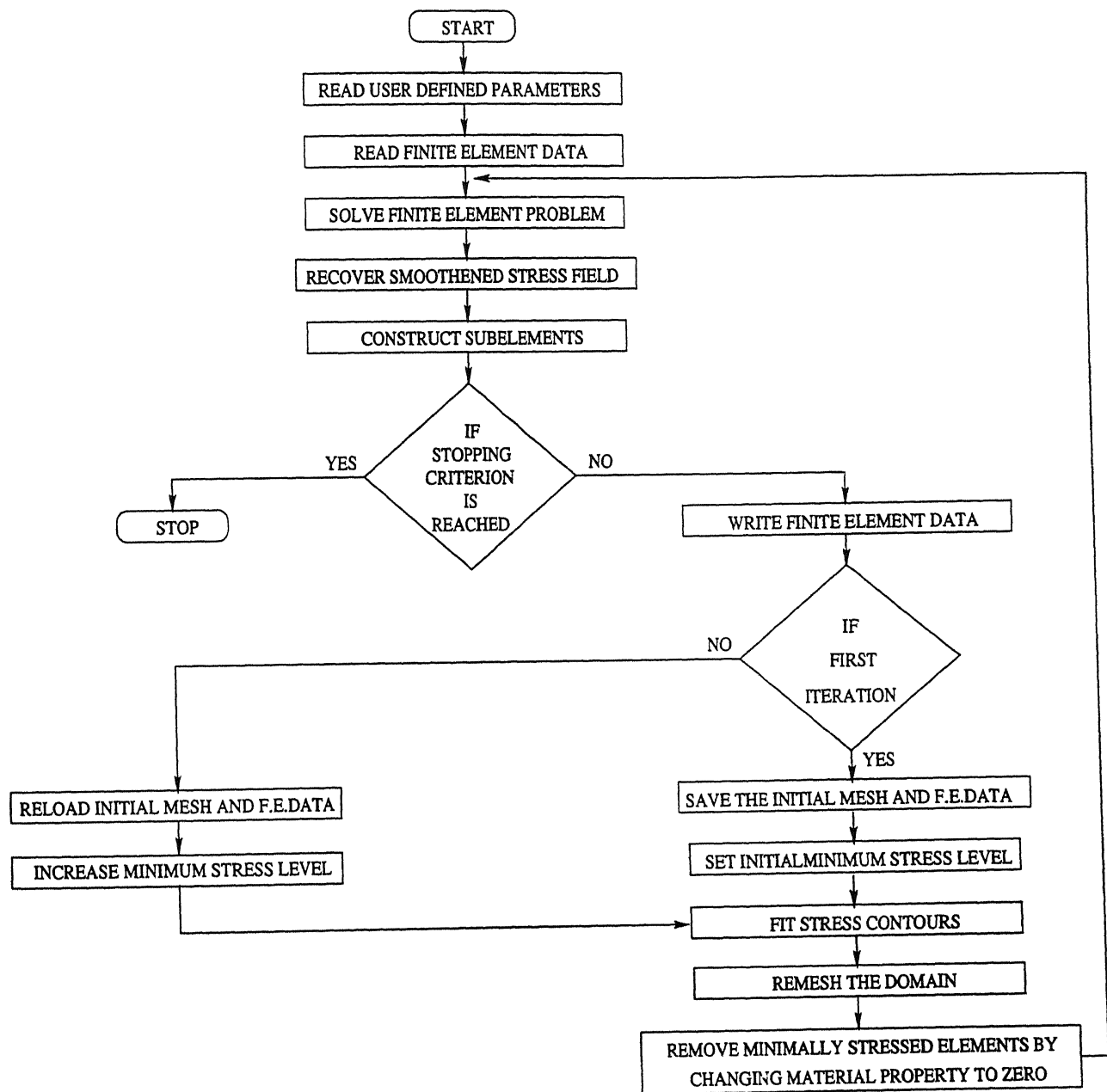
Figure 5.2: Flowchart for stiffener design

4 divisions in x-axis and 4 divisions in y-axis
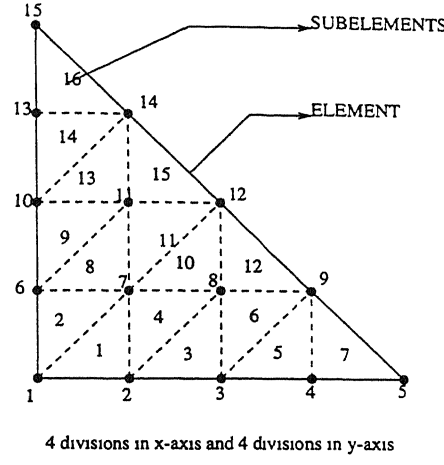
Figure 5.3: Subelements in a master element

is solved and smoothened stress field is recovered in postprocessing. The elements are then divided into subelements(see Fig.5.3) based on user specified divisions in x and y axis.The stress values at the vertices of the subelements are obtained using

$$
\begin{Bmatrix} \sigma_x \\ \sigma_y \\ \tau_{xy} \\ \tau_{yz} \\ \tau_{xz} \end{Bmatrix} = \sum_{i=1}^{NN} N_i^l \begin{Bmatrix} \sigma_{xi} \\ \sigma_{yi} \\ \tau_{xyi} \\ \tau_{yzi} \\ \tau_{xzi} \end{Bmatrix} \tag{5.1}
$$

$$
\{\sigma\} = \sum_{i=1}^{NN} N_i^l \{\sigma_i\} \tag{5.2}
$$

where, NN is the number of nodes in an element, N_i^l is the Lagrangian shape function associated with i^{th} node in terms of normalised coordinates ξ and η and $\{\sigma_i\}$ is the generalized stress vector corresponding to i^{th} node of an element. The element subdivision is carried in order to improve the accuracy of the identification of the low stressed material.

A maximum cutoff value for stress is set for each lamina with respect to its corresponding yield stress. Von Mises stress is calculated at each subelement nodes using

$$
(\sigma)_{Mises} = \left(\frac{1}{2} \left((\sigma_x - \sigma_y)^2 + \sigma_y^2 + \sigma_x^2 \right) + 3\tau_{xy}^2 + 3\tau_{yz}^2 + 3\tau_{xz}^2 \right)^{\frac{1}{2}} \tag{5.3}
$$

31

The acceptable design will be the one for which the Mises stress does not exceed the cut-off value at any point. Consider a lamina as shown in figure 5.4, For each node, the Mises stress is found at top,middle and bottom points of that lamina and the maximum value of those three points is stored for that node. If Mises stress values exceeds maximum cutoff value then stopping criterion is reached and the program is terminated. The finite element solution and mesh data of this initial configuration of stiffened plate is stored and evolutions are done using this data.
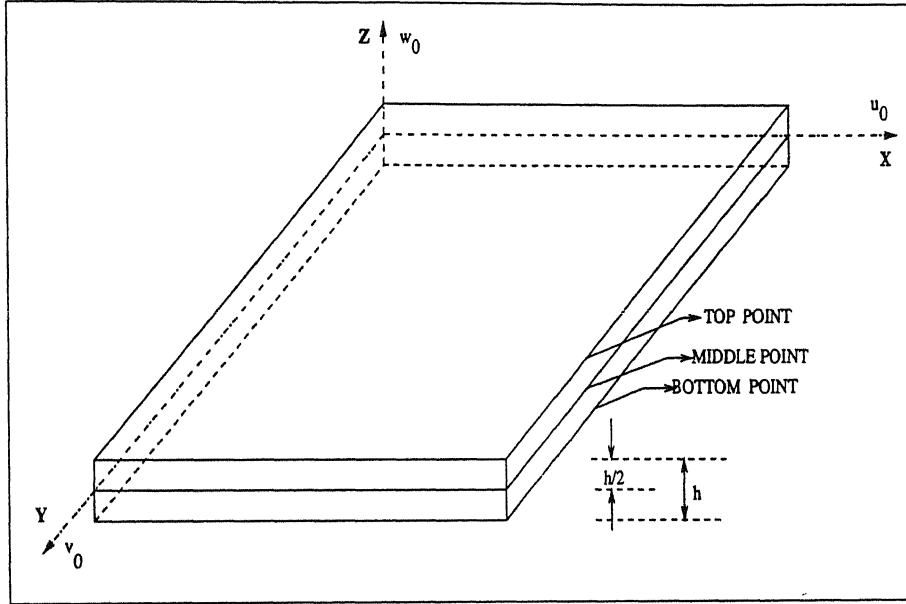
Figure 5.4: A lamina with points defined

For further evolution, the skin is untouched to maintain its external shape. Minimum cutoff value for stress is set with respect to yield stress for the stiffener such that the material in the regions having stress values less than this cutoff value is removed. Here the removal of material from an evolving design is typically done by changing the material properties,usually the Young's modulus, to a near zero value, representing a softening of the material. The elements are said to be 'killed' by decreasing the material property to near zero. Material is removed iteratively from the minimally stressed regions in the stiffener layer. In this way, in all regions of the design the stress will eventually be within a certain value of the maximum, producing a nearly fully stressed structure. To promote further change in the topol-

ogy of stiffener in each and every evolution, the minimum cutoff value for stress is increased incrementally based on a user supplied value.

Stress contours are plotted for minimally and maximally stressed regions and regions are remeshed seperately and the procedure followed for plotting of stress contours and remeshing are given in the next section. Stress values at all the subelement nodes in the bottom laminate(stiffener) and the minimum cut off value are used to fit stress contours. The minimum stressed regions in stiffener are identified and the elements in that regions are 'killed' by decreasing the material property to near zero and in the other regions material properties are unchanged. Then this evolved structure is solved for and stopping criterion is checked. If stopping criterion is reached then further evolution is stopped else the finite element solutions and mesh data of our initial plate configuration is restored and minimum cutoff value for stress is increased. Then stress contours are plotted,regions are remeshed and the process is repeated.

5.3   FITTING OF STRESS CONTOURS

During the process of evolutionary optimization, at each step of the evolution stress contours, for a given stress level, are to be drawn in order to identify minimally and maximally stressed regions and then the different domains got after contouring are remeshed separately. Figure 5.5 shows a flowchart of the main stages in the process of fitting stress contours. The stages are listed below and described in detail below.

Tracing the boundaries

Polygons construction

Splines construction
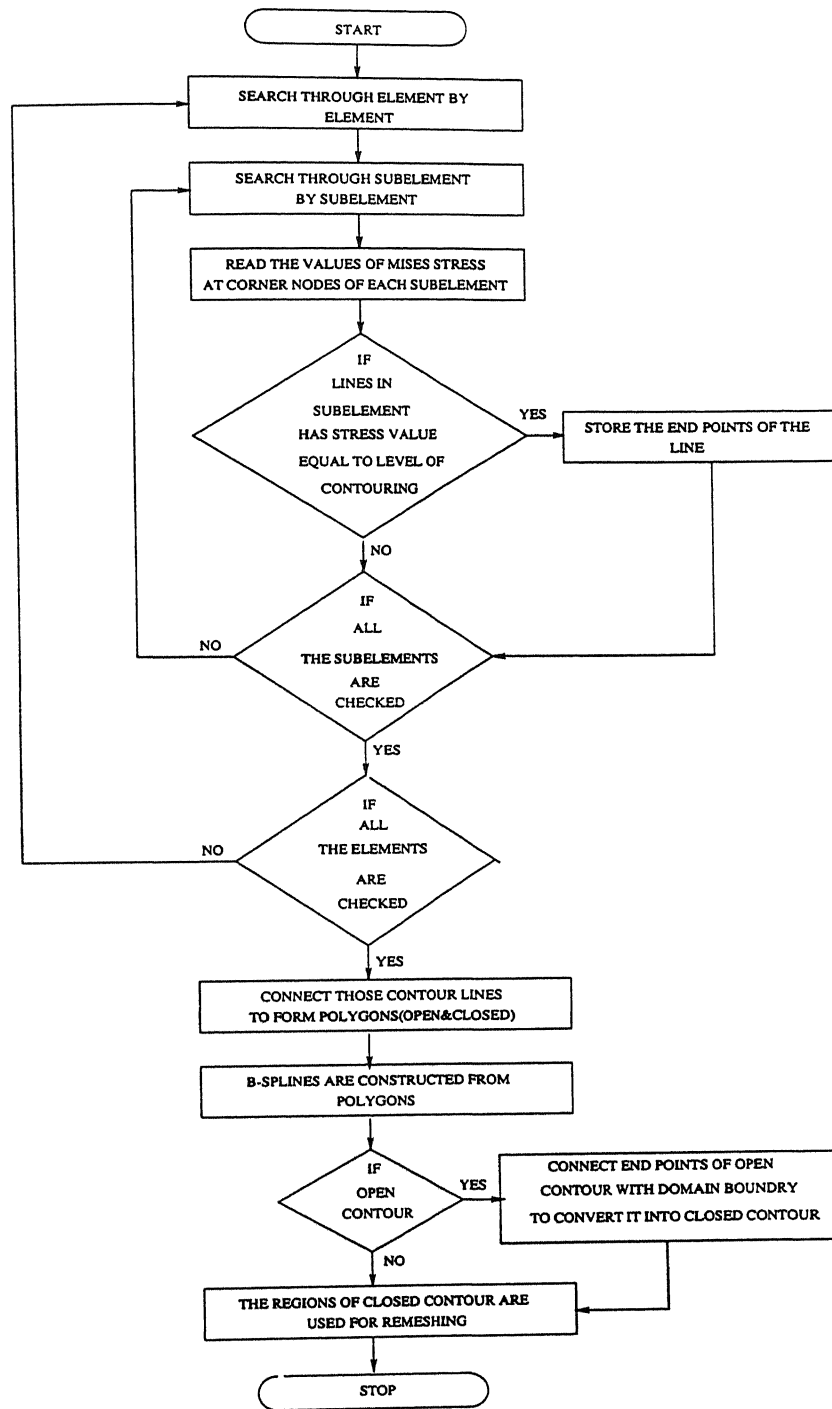
Regions separation and Remeshing

33

Figure 5.5: Flowchart for fitting of stress contours

34

5.3.1 TRACING THE BOUNDARIES

The initial step for fitting stress contours is to catch the boundary lines of minimally stressed regions in the stiffener. Steps followed for tracing the boundaries of minimally stressed regions are as follows

1. Loop over the subelements of each and every element.

2. Set the level of contouring for minimally stressed regions.

3. Load the von Mises stress for the three corner nodes of that subelement.

4. Checks are performed to find whether the subelement is having stress values, below the level of contouring or above the level of contouring or equal to the level of contouring or having stress values at some regions below the level of contouring and at some regions above the level of contouring.

5. If the subelement has stress values below or above level of contouring then that subelements are checked for whether it is lying on the domain boundaries of our plate. If true, then that line (edge of that subelement) endpoints are noted.

6. If the subelement has stress values equal to the level of contouring then the edge lines and endpoints of that element are noted.

7. If the subelement has stress values which are above the level of contouring at some nodes and at other nodes it has stress values less than the level of contouring, then interpolation is done to find out line passing through the subelements which has stress values equal to that of level of contouring and the end points of that line is noted.

8. After going through all elements we will get initial and final points of line segments of all the boundary contours of minimally stressed regions and also we will get the segmented lines of our plates domain boundary which are minimally and maximally stressed in separate files.

5.3.2 POLYGON CONSTRUCTION

From the continuity of stresses, there is a possibility of having only two types of contours(polygons).They are closed and open contours. Closed contours will have

boundaries which will be totally inside the plate domain boundaries or it can start and end at the same point on a domain boundary of the plate. Open contours will have their end points on plates domain boundaries but at different locations. These two types of contours are separately identified. First we start with open contours,by identifying the end points on boundaries and start connecting the segmented lines in that element and then identifying its continuity in its neighbor element,like this search goes and connects each and every opencontours seperatly.Then the search jumps into connecting closed contours by starting with a line segment in a element in which the contour is passing and continuing in the same way till all the closed contours are separately connected.

The boundary line segments are also connected to get boundary lines which are minimally and maximally stressed seperately.The following figure 5.6 shows how the boundaries are traced.
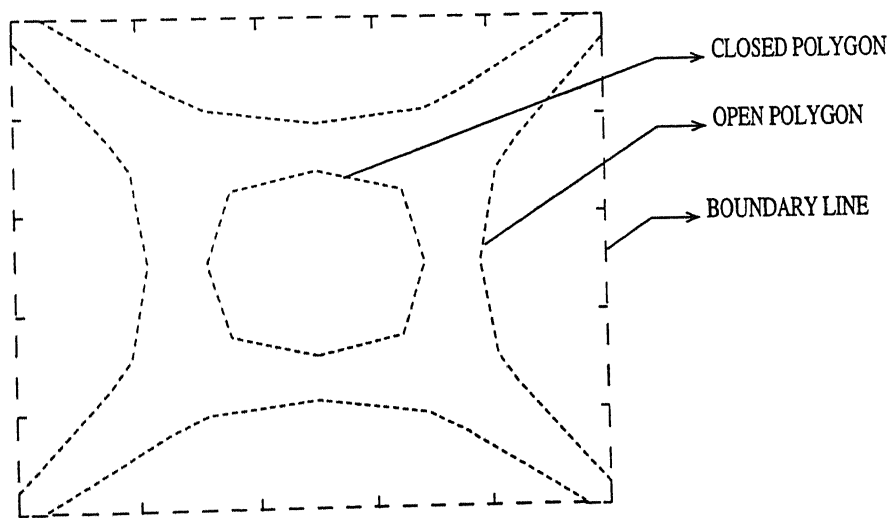
Figure 5.6: Showing boundary plots of various contours before spline construction
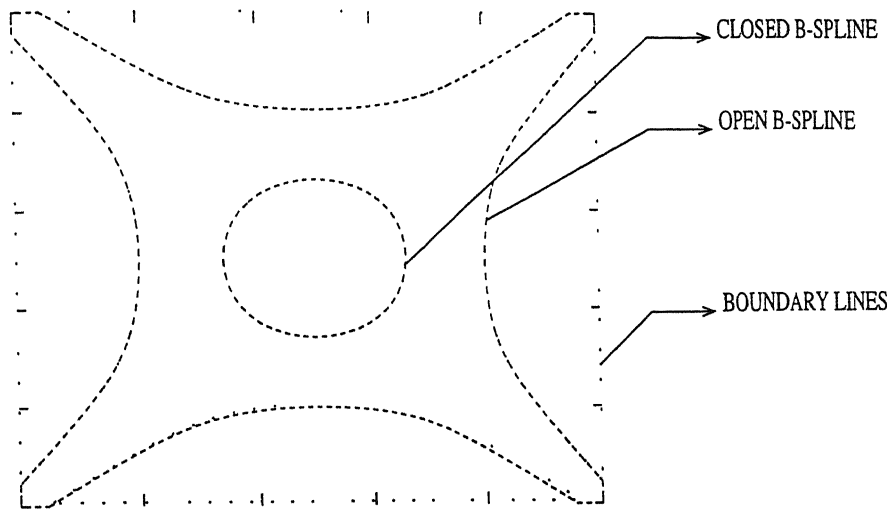
Figure 5.7: Showing boundary plots of various contours after spline construction

5.3.3 SPLINE CONSTRUCTION

Introduction

The techniques for generating curves are of two types, the first one is the curve fitting technique. In this, the curve generation is constrained such that the curves pass through existing data points. This is particularly suited to shape description, where the basic shape is arrived at by experimental evaluation or mathematical calculations. Examples are aircraft wings, engine manifolds, mechanical and or structural parts. The alternative method uses free form of curves and surfaces which is suited for another class of shape design problems that depends on both aesthetic and functional requirements. Examples are 'skin' of car bodies, aircraft fuselages, ship hulls, furnitures and glass ware. One form of generating free form of curves is B-splines.

B-spline curves

From a mathematical point of view a curve generated by using the vertex of a defining polygon is dependent on some interpolation or approximation scheme

to establish the relationship between the curve and the polygon. This scheme is provided by the choice of basis function.

Here the B-spline basis(or polynomial approximation function) is generally non global. The nonglobal behaviour of B-spline curves is due to the fact that each vertex is associated with unique basis function. Thus each vertex affects the shape of a curve only over a range of parameter values where its associated basis function is nonzero. The B-spline basis (see [10]) also allows the order of the basis function and hence the degree of the resulting curves to be changed without changing the number of defining polygon vertices.

The equation for B-spline curves can be expressed in a matrix form for both open and closed periodic B-spline curves. A open periodic B-spline curve is given by

$$P_j(t^*) = [T^*][N^*][G] \qquad 1 \leq j \leq n-k+1, \ 0 \leq t^* < 1 \qquad (5.4)$$

where here

$$[T^*] = [t^{*k-1} \ t^{*k-2} \ .... \ 1] \qquad 0 \leq t^* < 1$$

$$[G]^T = [B_j \ B_{j+1} \ B_{j+2} \ ... \ B_{j+(k-1)}]$$

$$N^*_{i+1,m+1} = \frac{1}{(k-1)!} \begin{pmatrix} k-1 \\ i \end{pmatrix} \sum_{l=m}^{k-1}(k-(l+1))^i(-1)^{l-m} \begin{pmatrix} k \\ l-j \end{pmatrix} \qquad (5.5)$$

$$0 \leq i,m \leq k-1$$

A closed periodic B-spline curve is given by

$$P_j(t^*) = [T^*][N^*][G] \qquad 0 \leq j \leq n, \ 0 \leq t^* < 1 \qquad (5.6)$$

where here

$$[T^*] = [t^{*k-1} \ t^{*k-2} \ .... \ 1] \qquad 0 \leq t^* < 1$$

$$[G]^T = [B_{(j \ mod \ (n+1))+1} \ B_{((j+1) \ mod \ (n+1))+1} \ ... \ B_{((j+1+n-k) \ mod \ (n+1))+1}]$$

$$(5.7)$$

$$N^*_{i+1,m+1} = \frac{1}{(k-1)!} \begin{pmatrix} k-1 \\ i \end{pmatrix} \sum_{l=m}^{k-1}(k-(l+1))^i(-1)^{l-m} \begin{pmatrix} k \\ l-j \end{pmatrix}$$

$$0 \leq i,m \leq k-1$$

38

In the above expressions for open and closed B-spline curves B_j are the position vectors of the n+1 defining polygon vertices and k represents the order of the B-spline curve. Formally a B-spline curve is defined as a polynomial spline function of order k (degree k-1) since it satisfies the following two conditions:

1. The function $P(t^*)$ is a polynomial of degree k-1 on each interval $0 \leq t^* < 1$

2. $p(t^*)$ and its derivatives of order 1,2,3,.....,k-2 are all continuous over the entire curve.Thus a fourth order is a piecewise cubic curve.

Thus the output files from polygons construction which contains the vertex points of the polygons are fed into splines construction routine. Corresponding to open or closed polygon,open or closed splines are constructed. The degree of the curves generated are controlled by the user. Figure 5.7 shows the contours after spline construction.

5.3.4 REGIONS SEPARATION AND REMESHING

The open splines are connected to minimally stressed boundary lines to form closed minimally stressed regions,the same open splines are connected with maximally stressed boundary lines to form closed maximally stressed regions.The closed contours are checked to find out which side of the closed contour is minimally stressed. Figure 5.8 shows how the regions are getting separated after spline construction. The main aim in regions separation is not to disturb the boundaries, if boundaries are distorted then we can't proceed further for remeshing.

Before proceeding to remeshing certain prerequisites are to be made to the output files which contains the seperated regions.

1. The data contained in each file which represents the individual regions should be arranged in such a way that when a contour is drawn using the data from starting to ending, it should proceed in anticlockwise direction. Measures are taken to identify whether the given data points in a file is in anticlockwise direction or in clockwise direction. If the data points are in clockwise direction it is reversed and made into anticlockwise direction. The procedure followed for identifying whether data
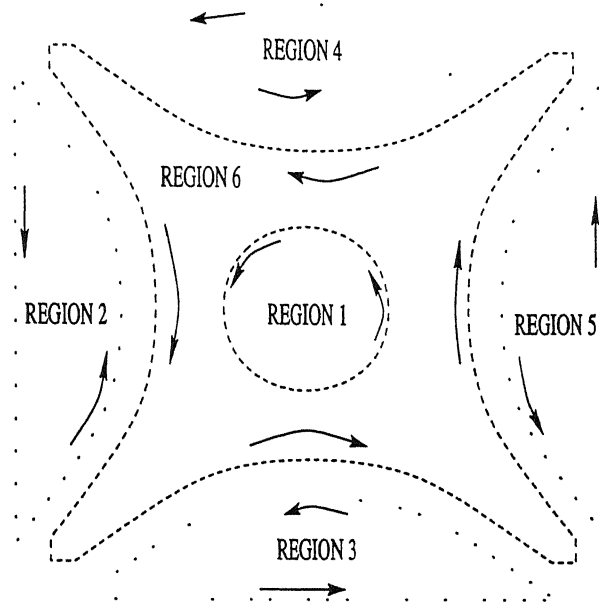
Figure 5.8: Showing seperated regions after spline construction

points are arranged in anticlockwise direction or not is given after this prerequisites discussion.

2. The files are to be arranged in such a way that the contours which are not enclosing closed contours are arranged first, then the contours which encloses closed contours are arranged next.

3. The contours which encloses closed contours to be provided with informations that how many contours are inside that contours and also in which files are their informations are available.

4. The data points in a file should be nearly equally spaced inorder to get elements of nearly equal sizes after remeshing.

Figure 5.8 shows for the case taken how are the regions getting arranged and how is the direction of the vectors in the data files. Remeshing is done in each and every regions and it will always mesh to the left of a vector so that finally every regions are meshed inside. To assist this behaviour vectors are fed in anticlockwise directions. Figure 5.9 shows the remeshed regions. The procedure for finding whether a set of data points contained in a file are arranged in anticlockwise or in clockwise direction is as follows

40

Figure 5.9: Remeshed regions

(a)
Anticlockwise contour
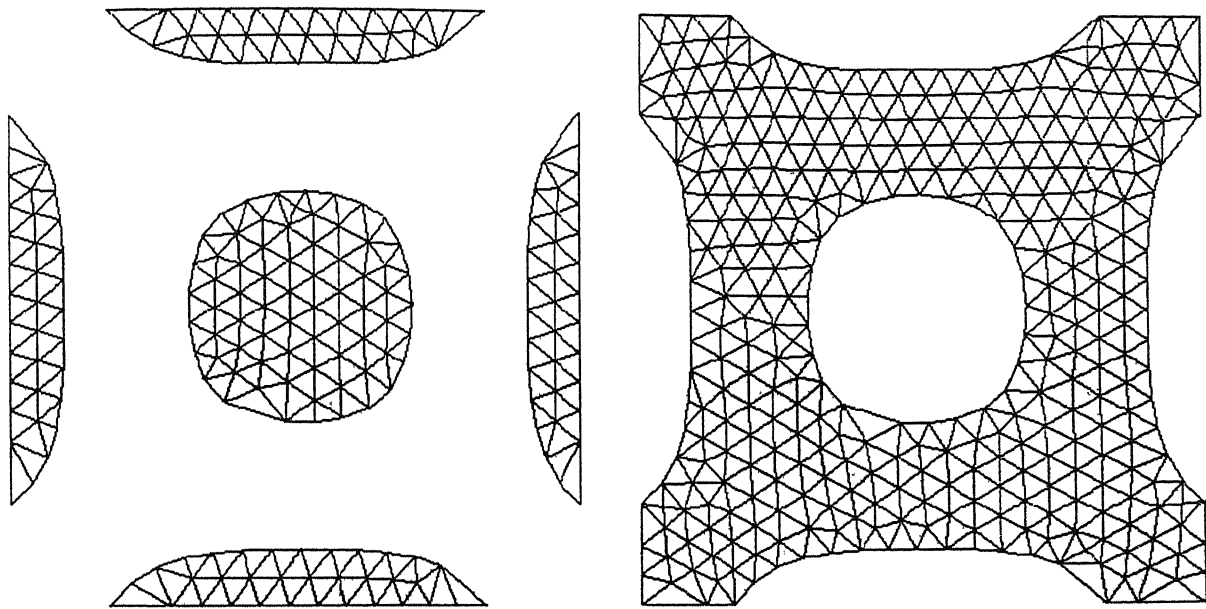
(b)
Clockwise contour
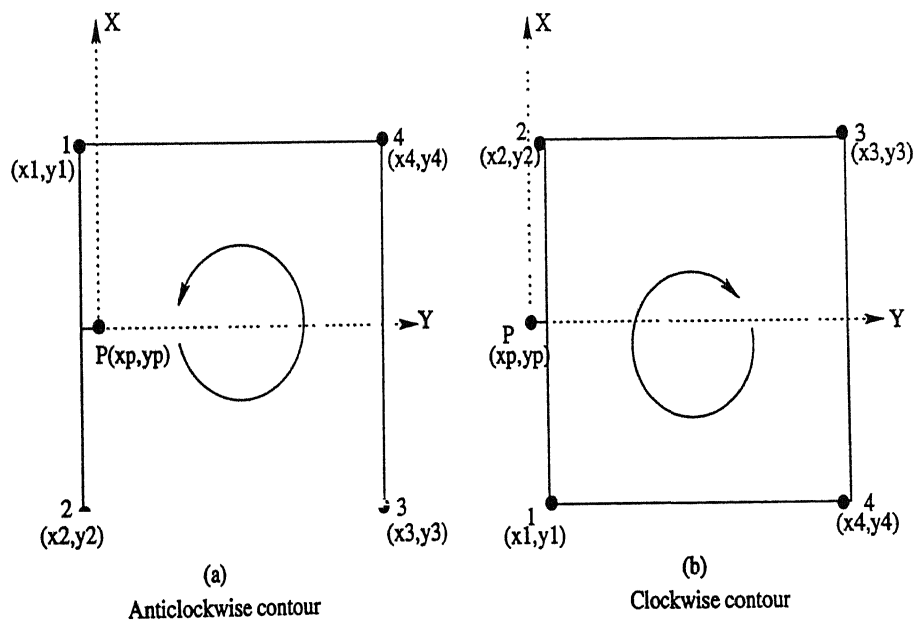
Figure 5.10: Showing clockwise and anticlockwise contours

1. The first point (x_1, y_1) and second point (x_2, y_2) from the data file is taken, these points represents a line segment. A inward normal(P) which is passing through midpoint of the linesegment is found using

$$P = \left(\frac{x_1 + x_2}{2} - 0.001(y_2 - y_1) \right) i + \left(\frac{y_1 + y_2}{2} + 0.001(x_2 - x_1) \right) j \qquad (5.8)$$

2. The inward normal(P) is shown in the figure for anticlockwise contour(5.10(a)) and for clockwise contour(5.10(b)). The point x_p and y_p are given as

$$x_p = \left(\frac{x_1 + x_2}{2} - 0.001(y_2 - y_1) \right) ; y_p = \left(\frac{y_1 + y_2}{2} + 0.001(x_2 - x_1) \right) \qquad (5.9)$$

3. X-axis and Y-axis is taken at the point $P(x_p, y_p)$ as shown in the figure.

4. The angle included between the points 1 and 2 with respect to point P is found, similarly angles included between points 2 and 3 with respect to point P is found and gets added with initial one and this process continues till the angle included between last point and first point is added.

5. The final included angle of the contour with respect to point $P(x_p, y_p)$ turns out to be 360 degrees for anticlockwise contours and it is zero for clockwise contours.

Chapter 6

NUMERICAL EXAMPLES

6.1 PLATE GEOMETRY

Figure 6.1: Stiffened plate geometry

A laminated plate of the dimesions as shown in fig. (6.1) has been considered for analysis.
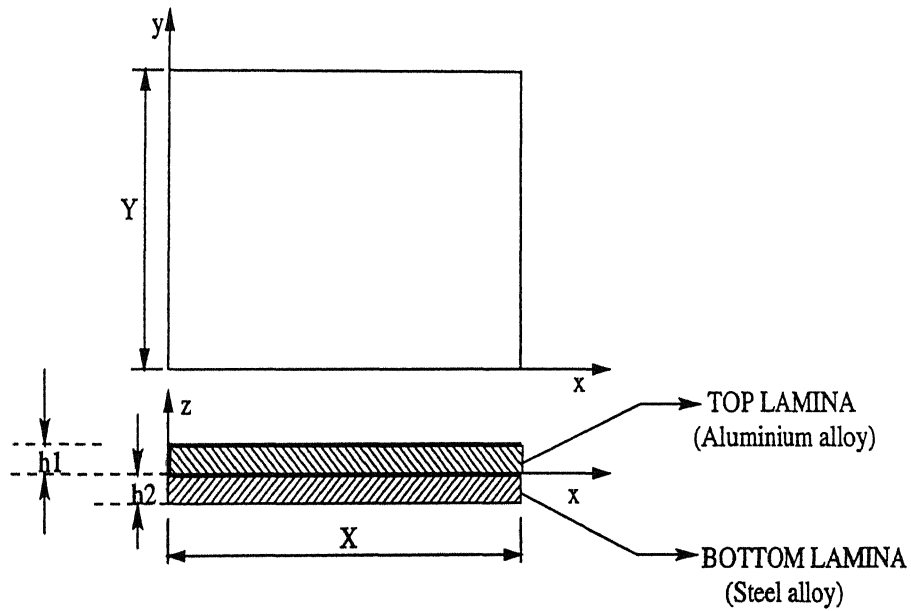
The plate is loaded transversely on the upper surface with the sinusoidal load:

$$q_z(x,y) = -q_c \, \sin(\frac{m \pi x}{X}) \, \sin(\frac{n \pi y}{Y}) \qquad (6.1)$$

The maximum cut-off value for stress is set as 80% of Yield stress of its corresponding material. The acceptable design will be the one for which the Mises stress does not exceed the maximum cut-off value at any point.

The material properties for the top aluminium lamina are as follows:

1. Yield stress(σ_y) = $406.8110174 N/mm^2$

2. Youngs modulus(E) = $72.3985709 \times 10^3 N/mm^2$

3. Rigidity modulus(G) = $27.58040796 \times 10^3 N/mm^2$

4. Poissons ratio(ν) = 0.33

5. Density(ρ) = $2794.576 \times 10^{-9} Kg/mm^3$

The material properties for the bottom steel lamina are as follows:

1. Yield stress(σ_y) = $1213.53795 N/mm^2$

2. Youngs modulus(E) = $199.9579 \times 10^3 N/mm^2$

3. Rigidity modulus(G) = $75.84612189 \times 10^3 N/mm^2$

4. Poissons ratio(ν) = 0.3

5. Density(ρ) = $7830.34 \times 10^{-9} Kg/mm^3$

The boundary conditions used are simply supported and clamped edges. The degrees of freedom fixed are shown in table 6.1 and 6.2.

Simply Supported	Clamped Edge
$w_0 = 0$	$w_0 = 0$
$u_0 = \theta_x = \psi_x = 0$	$u_0 = \theta_x = \psi_x = 0$
	$v_0 = \theta_y = \psi_y = 0$

Table 6.1: Boundary Conditions on x edge (y = constant)

Simply Supported	Clamped Edge
$w_0 = 0$	$w_0 = 0$
$v_0 = \theta_y = \psi_y = 0$	$u_0 = \theta_x = \psi_x = 0$
	$v_0 = \theta_y = \psi_y = 0$

Table 6.2: Boundary Conditions on y edge (x = constant)

PROBLEM 1

Four sides simply supported square laminated plate under sinusoidal transverse load on the top of the plate is analysed. The initial plate dimensions and load values are given below:

$X = 5\,mm;\quad Y = 5\,mm;$

$h1 = 0.5\,mm;\quad h2 = 0.04\,mm;$

$q_c = 21N/mm^2;\ \mathrm{m} = 1\ ;\ \mathrm{n} = 1$

Shape functions of order 2 was used.

Here the load taken is failure load for $0.5\,mm$ thick aluminium plate without any stiffener and the problem is to find suitable stiffener design so that the plate does not yield and also stiffener is optimized to give minimum weight configuration. The thickness of steel plate is taken as $0.04\,mm$ since at $0.03\,mm$ the plate fails in the initial configuration itself. Here the material removal is done starting from minimum cutoff value of 10% of yieldstress of steel plate. At each iteration it is increased by 1%. The plate is safe till the minimum cutoff value reached 33% of yieldstress of steel plate. It was noted that if the material removal is increased by increasing minimum cutoff value to 34% of yield stress of steel lamina, the Mises stress in the top lamina exceeded the maximum cut-off value set for it. Since the problem is symmetric, quarter plate analysis was done and figures of quarter plate is given in figure 6.2. The figure 6.2(a) shows the top aluminium laminas stress profiles before material is removed from bottom steel lamina and figure 6.2(c) shows the stress profiles of top aluminium lamina after material was removed from the regions which are below or equal to 33% of yield stress of steel from the steel lamina. Figure 6.2(b) and 6.2(d) shows the stress profiles of bottom steel lamina before and after material was removed.

The area of stiffener before material was removed $= 25mm^2$

The area of stiffener after material was removed $= 16.8434017mm^2$

Percentage of weight saved in stiffener $= 32.626\%$

Figure 6.2: Showing stress profiles for four sides simply supported square laminated plate(Quarter plate)

PROBLEM 2

Four sides clamped square laminated plate under sinusoidal transverse load on the top of the plate is analysed. The initial plate dimensions and load values are given below:

$X = 5\,mm;\quad Y = 5\,mm;$

$h1 = 0.5\,mm;\quad h2 = 0.0507\,mm;$

$q_c = 23N/mm^2;\ m = 1\ ;\ n = 1$

Shape functions of order 2 was used.

Here the load taken is failure load for 0.5 mm thick aluminium plate without any stiffener and the problem is to find suitable stiffener design so that the plate does not yield and also stiffener is optimized to give minimum weight configuratton. The thickness of steel plate is taken as 0.0507 mm since at 0.03 mm the plate fails in the initial configuration itself, and from 0.04 to 0.0506 mm the material removal is not significant. Here the material removal is done starting from minimum cutoff value of 5% of yieldstress of steel plate. At each iteration it is increased by 1%. The plate is safe till the minimum cutoff value reached 10% of yieldstress of steel plate. It was noted that if the material removal is increased by increasing minimum cutoff value to 11% of yield stress of steel lamina, the Mises stress in the top lamina exceeded the maximum cut-off value set for it. Since the problem is symmetric quarter plate analysis was done and figures of quarter plate is given in figure 6.3. The figure 6.3(a) shows the top aluminium laminas stress profiles before material is removed from bottom steel lamina and figure 6.3(c) shows the stress profiles of top aluminium lamina after material was removed from the regions which are below or equal to 10% of yield stress of steel from the steel lamina. Figure 6.3(b) and 6.3(d) shows the stress profiles of bottom steel lamina before and after material was removed.

The area of stiffener before material was removed $= 25mm^2$

The area of stiffener after material was removed $= 24.1316381mm^2$

Percentage of weight saved in stiffener $= 3.473\%$

Top Plate

INITIAL CONFIGURATION
(before material removal)

Bottom Plate
(Black regions are removed)

(a)

(b)

FINAL CONFIGURATION
(after material was removed)

(c)

(d)

WHITE REGIONS - Represents stress levels which are 65-80% of Yield stress of their corresponding material
LIGHTGREY REGIONS - Represents stress levels which are 45-65% of Yield stress of their corresponding material
GREY REGIONS - Represents stress levels which are 10-45% of Yield stress of their corresponding material
BLACK REGIONS - Represents stress levels which are 0-10% of Yield stress of their corresponding material

Figure 6.3: Showing stress profiles for four sides clamped square laminated plate(Quarter plate)

49

PROBLEM 3

A square laminated plate with two sides simply supported(at X = 0 and X = 5) and other two sides free, under sinusoidal transverse load on the top of the plate is analysed. The initial plate dimensions and load values are given below:

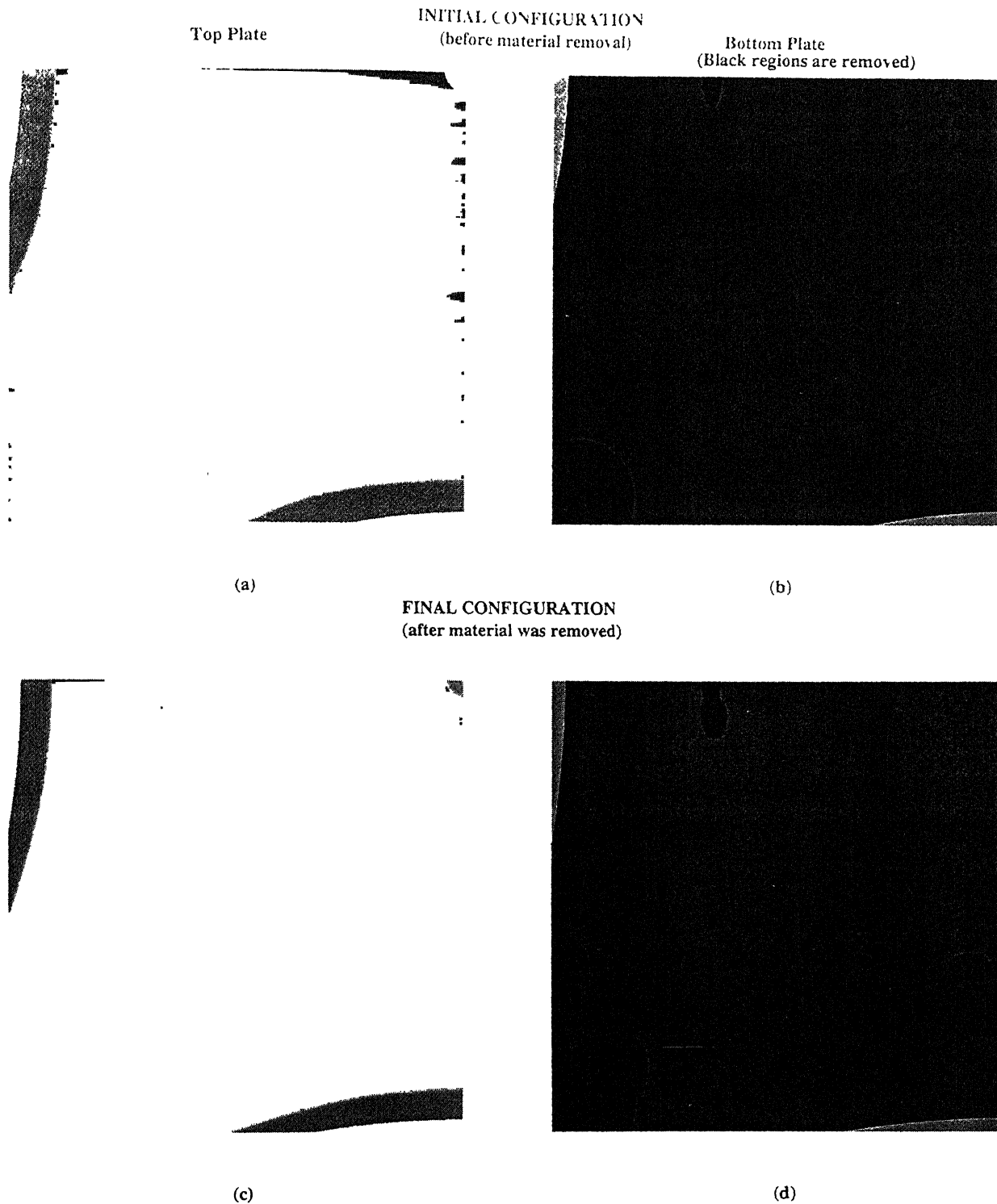$X = 5\,mm;\quad Y = 5\,mm;$

$h1 = 0.5\,mm;\quad h2 = 0.01\,mm;$

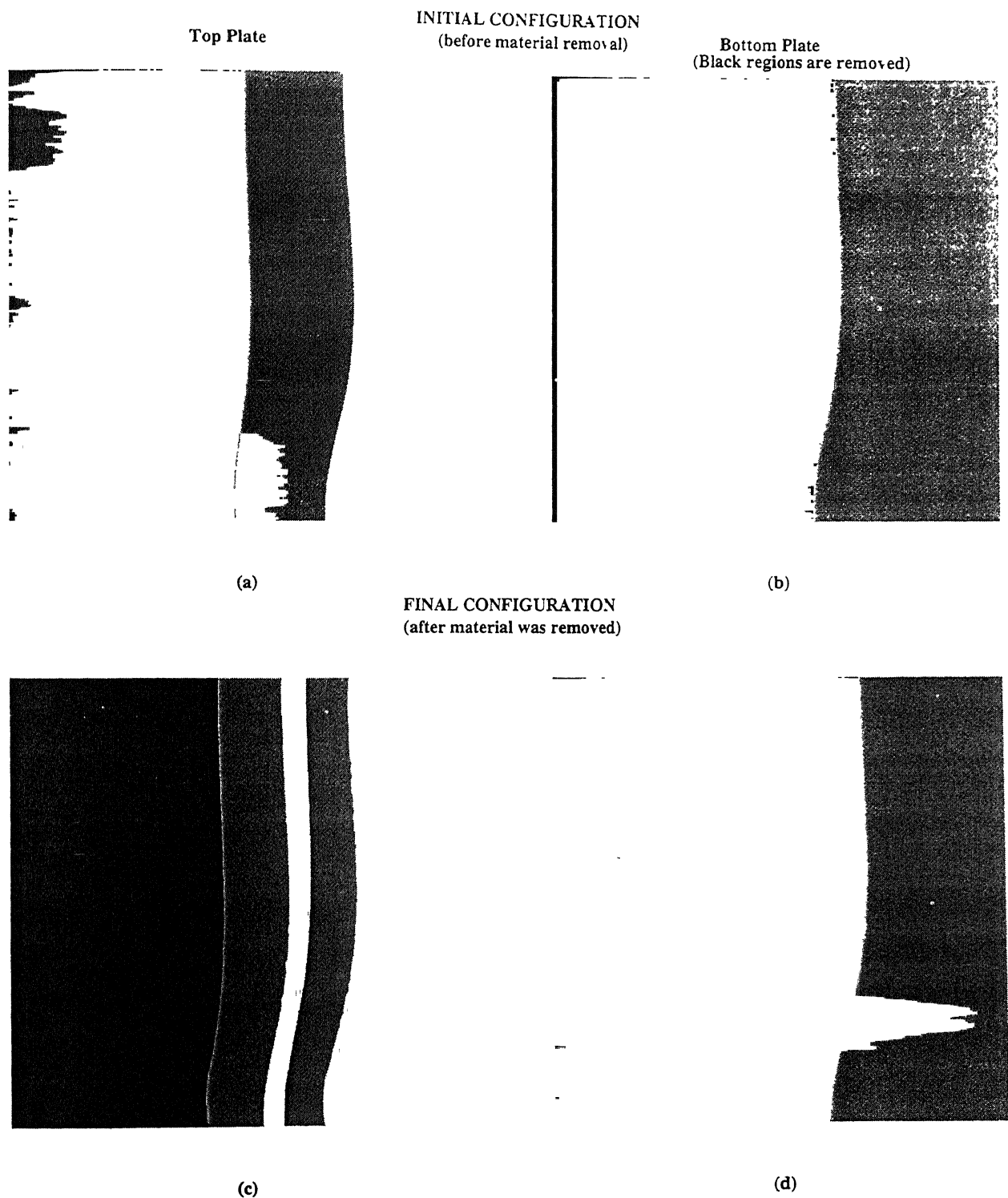$q_c = 9N/mm^2;\ m = 1\ ;\ n = 1$

Shape functions of order 2 was used.

Here the load taken is failure load for 0.5 mm thick aluminium plate without any stiffener and the problem is to find suitable stiffener design so that the plate does not yield and also stiffener is optimized to give minimum weight configuratton. The thickness of steel plate is taken as 0.01 mm . Here the material removal is done starting from minimum cutoff value of 10% of yieldstress of steel plate. At each iteration it is increased by 1%. The plate is safe till the minimum cutoff value reached 51% of yieldstress of steel plate. It was noted that if the material removal is increased by increasing minimum cutoff value to 52% of yield stress of steel lamina, the Mises stress in the top lamina exceeded the maximum cut-off value set for it. Since the problem is symmetric quarter plate analysis was done and figures of quarter plate is given in figure 6.4. The figure 6.4(a) shows the top aluminium laminas stress profiles before material is removed from bottom steel lamina and figure 6.4(c) shows the stress profiles of top aluminium lamina after material was removed from the regions which are below or equal to 51% of yield stress of steel from the steel lamina. Figure 6.4(b) and 6.4(d) shows the stress profiles of bottom steel lamina before and after material was removed.

The area of stiffener before material was removed = $25mm^2$

The area of stiffener after material was removed = $9.20863876mm^2$

Percentage of weight saved in stiffener = 63.1654%

Top Plate

INITIAL CONFIGURATION
(before material removal)

Bottom Plate
(Black regions are removed)

(a)

(b)

FINAL CONFIGURATION
(after material was removed)

(c)

(d)

WHITE REGIONS - Represents stress levels which are 65-80% of Yield stress of their corresponding material
GREY REGIONS - Represents stress levels which are 51-65% of Yield stress of their corresponding material
BLACK REGIONS - Represents stress levels which are 0-51% of Yield stress of their corresponding material

Figure 6.4: Showing stress profiles for two sides simply supported and two sides free square laminated plate(Quarter plate)

Chapter 7

CONCLUSIONS AND DISCUSSION

7.1 CONCLUSIONS

This study outlines an effective method to optimize stiffener topologies for plate structures. From the results obtained the following conclusions can be made

1. Recovery algorithms gives better and smoothened stress field as compared to the one obtained directly from the finite element solution.This helps to improve the accuracy of results and also helps in plotting smooth stress contours, leading to smooth boundaries for the material regions.

2. Capability to plot smooth contours of stress levels corresponding to a given threshold level using B-spline curves, removes the possibility of spurious corners being formed after material is removed.

3. Capability of remeshing removes the possibility of 'wrong' elements being removed. This remeshing algorithm also helps in changing the mesh size in each iteration according to users wish.

4. The algorithm does not starts with a very fine mesh. The number of elements tends to increase during the evolution and hence it is computationally more efficient.

5. The stiffener topologies depend on the type of boundary conditions and type of

loading conditions applied. Here it is shown that for change in boundary conditions not only the shape of the stiffener changes but also the thickness of stiffners also changes. From this, one should note that, to get a good design one should change both the thickness of the lamina and the stress levels.

6. The algorithm proceeds in a semi-automatic way to help user to control the process according to the results obtained in the previous step.

7.2 FUTURE WORK

1. For a given mesh,element order p, laminate properties, transverse loads, our finite element program gives the solution corresponding to our plate model. However, inorder to make this code more effective the following modules need to be developed:

   (a) A-posteriori error estimation for both discretization and modelling error.

   (b) Adaptivity based on error estimation to get the optimal rate of convergence for the discretisation error, for any data of interest.

   (c) Curved element mapping to represent curved boundaries.

   (d) Refinement of mesh on the boundaries of contours, to minimize the discretization errors, instead of refining the mesh for the whole domain.

2. Modules for applying different kinds of loading conditions can be added.

3. Modules for buckling analysis, free vibration problems, etc can be added.

4. The formulation can be generalized to curvilinear coordinates inorder to analyse shell structures.

5. Code can be extended to include geometric non-linearity to handle large deformations.

6. Instead of having single layer of stiffener, multilayered stiffeners can be optimized to get a 3-D profile for stiffeners.

7. Modules for shape optimization can be added to obtain the optimized shape for the cutouts obtained from topology optimization.

8. This method in principle is completely extendible to three dimensions without

any change except for the substitution of solid 3D elements for the 2D elements currently used.

.

APPENDIX A

$$\begin{Bmatrix} N_x \\ N_y \\ N_{xy} \\ M_x \\ M_y \\ M_{xy} \\ M_x^* \\ M_y^* \\ M_{xy}^* \\ Q_x \\ Q_y \\ Q_x^* \\ Q_y^* \end{Bmatrix} = \sum_{l=1}^{NL} \begin{bmatrix} [D_m]_{3\times3} & [D_c]_{3\times6} & [0]_{3\times4} \\ [D_c]_{6\times3}^T & [D_b]_{6\times6} & [0]_{6\times4} \\ [0]_{4\times3} & [0]_{4\times6} & [D_s]_{4\times4} \end{bmatrix}_l \begin{Bmatrix} \epsilon_x \\ \epsilon_y \\ \epsilon_{xy} \\ k_x \\ k_y \\ k_{xy} \\ k_x^* \\ k_y^* \\ k_{xy}^* \\ \nu_x \\ \nu_y \\ \nu_x^* \\ \nu_y^* \end{Bmatrix} \qquad (1)$$

where

$$[D_m]_l = \begin{bmatrix} \bar{Q}_{11}H_1 & \bar{Q}_{12}H_1 & \bar{Q}_{16}H_1 \\ \bar{Q}_{21}H_1 & \bar{Q}_{22}H_1 & \bar{Q}_{26}H_1 \\ \bar{Q}_{16}H_1 & \bar{Q}_{26}H_1 & \bar{Q}_{66}H_1 \end{bmatrix}_l$$

$$[D_c]_l = \begin{bmatrix} \bar{Q}_{11}H_2 & \bar{Q}_{12}H_2 & \bar{Q}_{16}H_2 & \bar{Q}_{11}H_4 & \bar{Q}_{12}H_4 & \bar{Q}_{16}H_4 \\ \bar{Q}_{21}H_2 & \bar{Q}_{22}H_2 & \bar{Q}_{26}H_2 & \bar{Q}_{11}H_4 & \bar{Q}_{12}H_4 & \bar{Q}_{16}H_4 \\ \bar{Q}_{16}H_2 & \bar{Q}_{26}H_2 & \bar{Q}_{66}H_2 & \bar{Q}_{11}H_4 & \bar{Q}_{12}H_4 & \bar{Q}_{16}H_4 \end{bmatrix}_l$$

$$[D_b]_l = \begin{bmatrix} \bar{Q}_{11}H_3 & \bar{Q}_{12}H_3 & \bar{Q}_{16}H_3 & \bar{Q}_{11}H_5 & \bar{Q}_{12}H_5 & \bar{Q}_{16}H_5 \\ \bar{Q}_{21}H_3 & \bar{Q}_{22}H_3 & \bar{Q}_{26}H_3 & \bar{Q}_{11}H_5 & \bar{Q}_{12}H_5 & \bar{Q}_{16}H_5 \\ \bar{Q}_{16}H_3 & \bar{Q}_{26}H_3 & \bar{Q}_{66}H_3 & \bar{Q}_{11}H_5 & \bar{Q}_{12}H_5 & \bar{Q}_{16}H_5 \\ \bar{Q}_{11}H_5 & \bar{Q}_{12}H_5 & \bar{Q}_{16}H_5 & \bar{Q}_{11}H_7 & \bar{Q}_{12}H_7 & \bar{Q}_{16}H_7 \\ \bar{Q}_{21}H_5 & \bar{Q}_{22}H_5 & \bar{Q}_{26}H_5 & \bar{Q}_{11}H_7 & \bar{Q}_{12}H_7 & \bar{Q}_{16}H_7 \\ \bar{Q}_{16}H_5 & \bar{Q}_{26}H_5 & \bar{Q}_{66}H_5 & \bar{Q}_{11}H_7 & \bar{Q}_{12}H_7 & \bar{Q}_{16}H_7 \end{bmatrix}_l$$

i

$$[D_s]_l = \begin{bmatrix} \bar{Q}_{55}H_1 & \bar{Q}_{45}H_1 & \bar{Q}_{55}H_3 & \bar{Q}_{45}H_3 \\ \bar{Q}_{45}H_1 & \bar{Q}_{44}H_1 & \bar{Q}_{45}H_3 & \bar{Q}_{44}H_3 \\ \bar{Q}_{55}H_3 & \bar{Q}_{45}H_3 & \bar{Q}_{55}H_5 & \bar{Q}_{45}H_5 \\ \bar{Q}_{45}H_3 & \bar{Q}_{44}H_3 & \bar{Q}_{45}H_5 & \bar{Q}_{44}H_5 \end{bmatrix}_l$$

in which,

$$H_i = \frac{1}{i}\left(t^i_l - t^i_{l-1} \right), \; i = 1,2,3,4,5,7$$

.

$$[N] = \begin{bmatrix} N_1 & 0 & 0 & ... & N_2 & 0 & 0 & ... \\ 0 & N_1 & 0 & ... & 0 & N_2 & 0 & ... \\ 0 & 0 & N_1 & ... & 0 & 0 & N_2 & ... \\ \vdots & & & & \vdots & & \vdots & \end{bmatrix} \tag{1}$$

$$[B_m] = \begin{bmatrix} N_{i,x} & 0 & 0 & 0 & 0 & 0 & 0 \\ 0 & N_{i,y} & 0 & 0 & 0 & 0 & 0 \\ N_{i,y} & N_{i,x} & 0 & 0 & 0 & 0 & 0 \end{bmatrix} \tag{2}$$

$$[B_b] = \begin{bmatrix} 0 & 0 & 0 & N_{i,x} & 0 & 0 & 0 \\ 0 & 0 & 0 & 0 & N_{i,y} & 0 & 0 \\ 0 & 0 & 0 & N_{i,y} & N_{i,x} & 0 & 0 \\ 0 & 0 & 0 & 0 & 0 & N_{i,x} & 0 \\ 0 & 0 & 0 & 0 & 0 & 0 & N_{i,y} \\ 0 & 0 & 0 & 0 & 0 & N_{i,y} & N_{i,x} \end{bmatrix} \tag{3}$$

$$[B_s] = \begin{bmatrix} 0 & 0 & N_{i,x} & 1 & 0 & 0 & 0 \\ 0 & 0 & N_{i,y} & 0 & 1 & 0 & 0 \\ 0 & 0 & 0 & 0 & 0 & 3 & 0 \\ 0 & 0 & 0 & 0 & 0 & 0 & 3 \end{bmatrix} \tag{4}$$

$$\{d^T\} = \{\delta_1^T, \delta_2^T, ...\delta_{NN}^T\} \tag{5}$$

Bibliography

[1] Pandya B.N., Mallikarjuna and Kant T. *Ph. D. Dissertation at Indian Institute of Technology, Bombay, India. Private Publication.*

[2] Sharma H. "A Comparative Study of Averaging Schemes for the Periodic Heterogeneous Media."M.Tech Thesis at IIT Kanpur,Oct.2000.

[3] Maute K. and Ramm E. "Adaptive Topology Optimization." *Structural Optimization. Vol.10,1995 pp.100-112.*

[4] Reynolds D., McConnachie J., Bettess P., Christie W.C. and Bull J,W. " Reverse Adaptivity-A New Evolutionary Tool for Structural Optimization. "*International Journal for Numerical Methods in Engineering, Vol.45,1999 PP. 529-552.*

[5] Maute K. and Ramm E."Adaptive Topology Optimization of Shell Structures."*AIAA Journal, Vol.35,1997 pp.1767-1773.*

[6] Xie Y.M. and Steven G.P. " A Simple Evolutionary Procedure for Structural Optimization." *Computers and Structures, Vol.49,1993 PP.885-896.*

[7] Hinton E. and Suebz J. "Fully Stressed Toplological Design of Structures Using an Evolutionary Procedure." *Engineering computations, Vol.11,1995 pp.229-244.*

[8] Agarwal B.D. and Broutman L.J. Analysis and Performance of Fiber Composites. John Wiley and Sons, New Delhi.

[9] Jones R.M. Mechanics of Composite Materials. Scripta Book Company, McGraw- Hill Kogakusha, Ltd. New Delhi.

[10] Rogers D.F. and Adams J.A. Mathematical Elements for Computer Graphics. McGraw-Hill Publishing Company. 1990.

[11] Cox M.G. "The Numerical Evaluation of B-Splines." *National Physical Laboratory DNAC 4,August 1971.*

[12] de Boor and Carl. "On Calculation with B-Splines." *J.Approx.Theory, Vol.6,1972 PP.50-62.*

[13] Mohite P.M. " Adaptive Finite Element Based Shape Optimization of Laminated Composite Plates with Cut-outs." M.Tech Thesis at IIT Kanpur,Feb.2001.

[14] Kikuchi N. and Bendsoe M.P. "Generating Optimal Topologies in Structural Design Using a Homogenization Method." *Computer Methods in Applied Mechanics and Engineering, Vol.71,1988 pp.197-224.*

[15] Kikuchi N. and Diaz A.R. "Solutions to Shape and Topology Eigenvalue Optimization Problems Using a Homogenization Method." *Int. J. for Numerical Methods in Engineering, Vol.35,1992 pp.1487-1502.*

[16] Schmit L.A. "Structural Synthesis-Its Genesis and Development" *AIAA journal, October 1981 pp.1249-1263.*

[17] Vanderplaats G.N. "Structural Design Optimization Status and Direction." *J. of Aircraft, Vol.36,1999 pp.11-20.*

[18] Vanderplaats G.N. "Structural Optimizaion-Past,Present, and Future." *AIAA Journal, Vol.20,1982 pp.992-1000.*

133655

Date Slip

The book is to be returned on
the date last stamped.

....	....
....	....
....	....
....	....
....	....
....	....
....	....
....	....
....	....
....	....
....	....
....	....